

Original paper

# Bismuth, lead–bismuth and lead–antimony sulfosalts from the granite-hosted hydrothermal quartz veins at the Elisabeth mine, Gemerská Poloma, Spišsko-gemerské rudoohorie Mts., Slovakia

Martin ŠTEVKO<sup>1,2\*</sup>, Jiří SEJKORA<sup>2</sup>

<sup>1</sup> Earth Science Institute, Slovak Academy of Sciences, Dúbravská cesta 9, 840 05 Bratislava, Slovak Republic; martin.stevko@savba.sk

<sup>2</sup> Department of Mineralogy and Petrology, National Museum, Cirkusová 1740, 193 00 Prague 9, Czech Republic

\* Corresponding author



An interesting assemblage of bismuth and complex lead–bismuth and lead–antimony sulfosalts have been identified in samples from hydrothermal quartz veins hosted in S-type granitic rocks at the Elisabeth mine near Gemerská Poloma, Slovakia. We provide the first detailed study of the chemical composition of sulfosalts from the hydrothermal veins directly related to the specialized (Sn–W–F enriched) Gemic granites. Bismuthinite derivates (bismuthinite and phases with  $n_{\text{aik}}$  ranging from 21.3 to 23.7 and 30.3), minerals of the kobellite–tintinaite series (with Sb/(Sb+Bi) atomic ratio ranging considerably between 0.13 and 0.71), giessenite–izoklakeite series (with Sb/(Sb+Bi) from 0.26 to 0.33) as well as Pb–Sb sulfosalts (mainly jamesonite, boulangerite, robinsonite and their Bi-rich varieties) are common. Rare Bi-enriched rouxelite, bournonite and minerals of the tetrahedrite group were also observed. The two distinct types of sulfosalts associations were distinguished, each related to the different type of host rock and with variable Bi/Sb ratio. The first is represented predominantly by Bi-rich sulfosalts (bismuthinite derivates, kobellite, giessenite–izoklakeite) and occurs in the quartz veins hosted in P-enriched leucogranite. The second association is developed only in hydrothermal quartz veins hosted in porphyric granites and except of Bi (bismuthinite derivates) also significant amounts of Sb-rich sulfosalts (tintinaite, boulangerite, robinsonite, jamesonite, rouxelite, bournonite and tetrahedrite-(Zn) to tetrahedrite-(Fe)) are present.

**Keywords:** sulfosalts, bismuthinite derivates, kobellite homologous series, rouxelite, S-type granite, Gemerská Poloma

Received: 26 May 2021; accepted: 1 October 2021; handling editor: J. Zachariáš

The online version of this article (doi: 10.3190/jgeosci.328) contains supplementary electronic material.

## 1. Introduction

The greisens, albitites and hydrothermal quartz veins related to specialized S-type Gemic granites were intensively explored for Sn, W, Mo, Nb, Ta and Li. Even though several interesting mineral associations were discovered (e.g., Malachovský et al. 1997, 2000; Petrik et al. 2011; Števko et al. 2015, 2018; Radvanec and Gonda 2019), the sulfidic ore mineralization and especially sulfosalts were never studied in detail. There are only scattered reports about occurrence of bismuthinite, cosalite, jamesonite, emblectite, tetrahedrite and garavallite from greisens and related hydrothermal quartz veins at the Medvedí potok Sn–W–Mo deposit near Hnilec (Drnžíková and Mandáková 1982; Radvanec and Gonda 2019). Malachovský (1983) described the occurrence of bismuthinite, kobellite, Bi-rich jamesonite and Bi-rich boulangerite from greisens and hydrothermal quartz veins hosted in granite from Dlhá dolina near Gemerská Poloma.

This paper is focused on the detailed mineralogical characterization of recently discovered association of bismuth, lead–bismuth and lead–antimony sulfosalts from

the hydrothermal quartz veins hosted in a hidden intrusion of S-type Gemic granites at the Elisabeth mine near Gemerská Poloma. New data on the chemical composition of minerals of the bismuthinite–aikinite series, kobellite homologous series, Pb–Sb sulfosalts and rouxelite as well as their paragenetic relations are presented.

## 2. Geological setting

The hydrothermal quartz veins with sulfosalts, sulfides, carbonates and phosphates are hosted in the hidden intrusion of specialized Gemic granites, which was recently uncovered during the excavation of Elisabeth adit at the Gemerská Poloma talc deposit, located about 10 km northwest of Rožňava town, Spišsko-gemerské rudoohorie Mts., Slovak Republic [GPS 48°45'4.07"N and 20°29'39.32"E].

The granitic rocks of the Gemic Unit represent a distinct type of specialized (Sn–W–F), highly evolved suite with S-type affinity that differs from other granitoids occurring in the Veporic and Tatic Units of the Western Carpathian crystalline basement. Besides fluorine, they

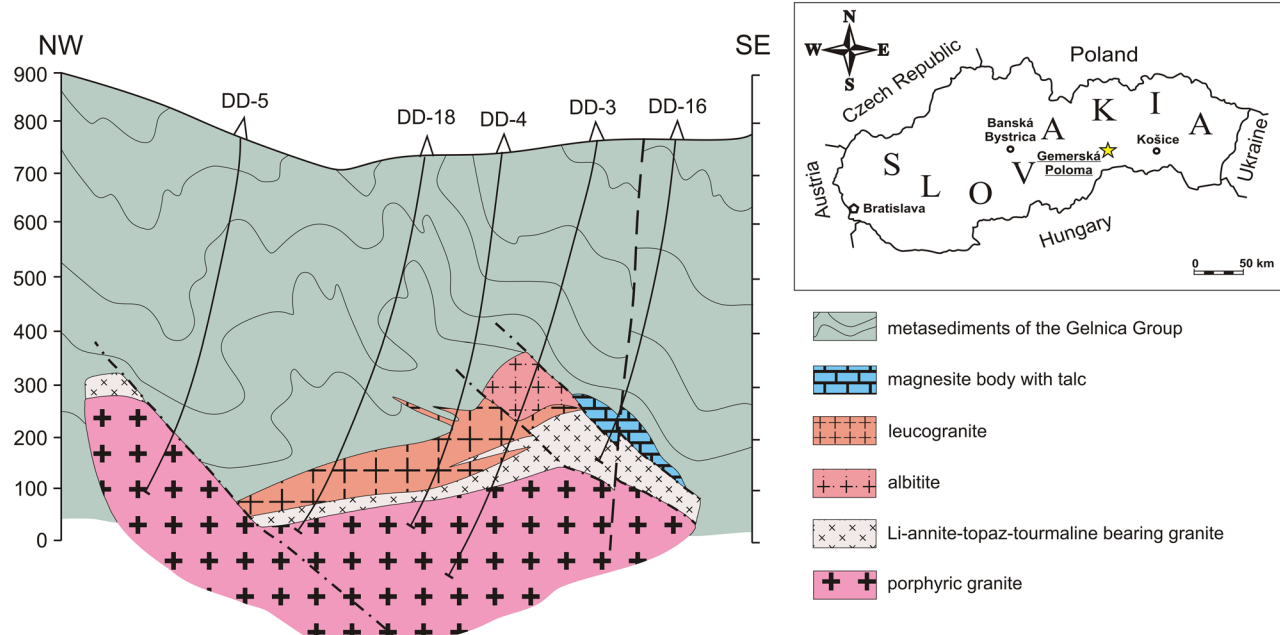


**Fig. 1** Cross section of the granite pluton and talc deposit near Gemerská Poloma (modified after Dianiška et al. 2002).

are enriched in phosphorus and rare lithophile elements, such as Li, Rb, Cs, B, Ga, Sn, W, Nb, Ta, U and depleted in REE, Zr, Ti, Sr, Ba (e.g., Uher and Broska 1996; Petrik and Kohút 1997; Broska and Uher 2001; Kubiš and Broska 2005, 2010; Broska and Kubiš 2018; Villaseñor et al. 2021). Recent zircon U–Pb and molybdenite Re–Os isotopic dating indicate emplacement of the Gemic granites and related post-magmatic mineralization during Late Permian (~260 to 230 Ma; Poller et al. 2002; Kohút and Stein 2005; Radvanec et al. 2009; Villaseñor et al. 2021). Younger, Alpine (Cretaceous) fluid-driven low-temperature tectono-metamorphic overprint affected the granitic rocks along mylonite zones (Breiter et al. 2015).

The Gemic granitic rocks form several small plutons intruding the intensively folded Lower Paleozoic (mainly Ordovician to Devonian) volcano-sedimentary complex of the Gelnica Group metamorphosed under greenschist-facies metamorphic conditions (Bajaník et al. 1984; Petrasová et al. 2007). In the studied area, the metamorphic rocks are represented mainly by phyllites, metapyroclastic rocks of rhyolitic to dacitic composition, locally with bodies and lenses of metadolomite and strongly stearitized magnesite. The latter has been recently exploited by Elisabeth mine as a talc deposit near Gemerská Poloma (Kilík 1997; Radvanec et al. 2004; Petrasová et al. 2007). Several types of granites were distinguished in the studied area (Fig. 1): (a) coarse-grained porphyric granite to granite porphyry, (b) medium-grained Li-annite–topaz–tourmaline bearing granite, (c) P-enriched topaz–zinnwaldite leucogranite and (d) albitite (Dianiška et al. 2002, 2007; Breiter et al. 2015). Except for

the albitites, all listed types of granitic rocks were recently found in the Elisabeth adit (Števko et al. 2015, 2018).

The hydrothermal quartz veins with sulfosalts were observed in all types of granitic rocks but are especially common in porphyric granites and P-enriched leucogranite. They are generally up to 15 cm thick and up to 3 m long. Besides sulfosalts, they contain variable amounts of albite, muscovite, Li-bearing micas, chlorites, rutile, fluorite, polycrase-(Y) to uranopolycrase, bastnäsite-(Ce), carbonates (Mn-rich siderite, rhodochrosite, calcite and dolomite), phosphates (fluorapatite, triplite, fluorarrojadite-(BaNa), fluorarrojadite-(BaFe), fluordickinsonite-(BaNa) and viitanniemiite) and sulfides like pyrite, arsenopyrite, sphalerite, chalcopyrite and minor galena (Uher et al. 2009; Števko et al. 2015, 2018, 2020).

### 3. Analytical methods

The samples with sulfosalts were systematically (period of 2009–2018) collected at the dumps of Elisabeth mine from the hydrothermal quartz veins hosted in various types of granitic rocks.

Quantitative chemical analyses of sulfosalts were performed on a Cameca SX100 electron microprobe (Department of Mineralogy and Petrology, National Museum, Prague, Czech Republic), operating in the wavelength-dispersive (WDS) mode (25 kV, 20 nA and 2 to 5 µm wide beam). The following standards and X-ray lines were used (DL – detection limit, in wt. %):

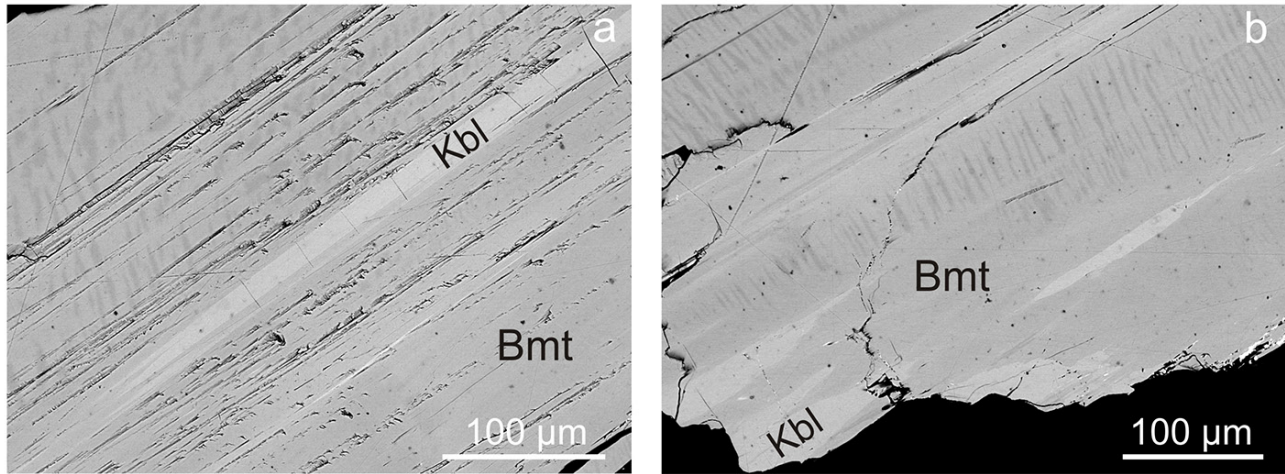


**Fig. 2a** – Bismuthinite (Bmt) associated with kobellite (Kbl). The darker ribbons in bismuthinite are phases fitting to the compositional gap between pekoite and gladite. Sample GPES2, BSE image. **b** – Exsolution lamellae and ribbons of phases fitting to the compositional gap between pekoite and gladite (dark grey) in bismuthinite (Bmt). Light grey elongated inclusions are kobellite (Kbl). Sample GPES2, BSE image.

Ag ( $\text{AgL}_\alpha$  DL 0.07), Bi ( $\text{BiM}_\beta$  DL 0.28), CdTe ( $\text{CdL}_\alpha$  DL 0.07), chalcopyrite ( $\text{CuK}_\alpha$  DL 0.05,  $\text{SK}_\alpha$  DL 0.05), halite ( $\text{ClK}_\alpha$  DL 0.04), HgTe ( $\text{HgM}_\alpha$  DL 0.27), InAs ( $\text{InL}_\alpha$  DL 0.05), Mn ( $\text{MnK}_\alpha$  DL 0.04), NiAs ( $\text{AsL}_\alpha$  DL 0.06), PbS ( $\text{PbM}_\alpha$  DL 0.11), PbSe ( $\text{SeL}_\beta$  DL 0.08), pyrite ( $\text{FeK}_\alpha$  DL 0.04),  $\text{Sb}_2\text{S}_3$  ( $\text{SbL}_\alpha$  DL 0.05), Sn ( $\text{SnL}_\alpha$  DL 0.05), PbTe ( $\text{TeL}_\alpha$  DL 0.06) and ZnS ( $\text{ZnK}_\alpha$  DL 0.06). Contents of the above-listed elements, which are not included in the tables, were analyzed quantitatively but were consistently below the detection limit. Raw intensities were converted to the concentrations of elements using automatic “PAP” matrix-correction software (Pouchou and Pichoir 1985).

**Tab. 1** Representative chemical analyses of bismuthinite derivates from Gemerská Poloma (in wt. %)

h.r.	GPES2				GPES3			GPES7		GPX1		GPA2		GPA8	
	LG				LG			PG		PG		PG		PG	
Pb	12.50	10.22	5.76	1.94	4.19	2.91	2.71	2.56	4.33	3.35	0.36	0.01	1.27	3.17	2.06
Cu	3.60	2.89	1.79	0.33	1.22	0.83	0.73	0.74	1.36	1.00	0.24	0.28	0.37	0.83	0.51
Sb	3.37	3.61	3.65	4.25	3.55	9.11	3.30	5.69	3.80	3.81	14.35	24.99	23.99	14.05	14.42
Bi	62.17	64.22	69.79	73.47	71.83	67.47	74.40	71.69	70.88	72.20	63.84	52.20	52.31	60.73	61.78
S	18.62	18.85	18.82	19.02	18.97	19.96	19.28	19.19	19.64	19.60	20.92	22.00	22.05	21.02	21.19
Se	0.18	0.18	0.22	0.20	0.22	0.00	0.32	0.26	0.15	0.10	0.00	0.00	0.00	0.00	0.00
Cl	0.00	0.00	0.00	0.00	0.00	0.00	0.12	0.00	0.00	0.00	0.00	0.00	0.00	0.00	0.00
total	100.44	99.97	100.03	99.21	99.97	100.28	100.86	100.13	100.16	100.06	99.70	99.47	99.99	99.80	99.98
Cu	1.181	0.947	0.575	0.106	0.392	0.254	0.232	0.232	0.436	0.322	0.032	0.000	0.108	0.250	0.153
Pb	1.258	1.027	0.567	0.190	0.412	0.273	0.265	0.246	0.427	0.329	0.069	0.076	0.102	0.291	0.188
Bi	6.203	6.396	6.817	7.143	7.005	6.280	7.203	6.830	6.931	7.037	2.213	3.591	3.477	5.532	5.590
Sb	0.577	0.617	0.612	0.709	0.594	1.456	0.548	0.931	0.637	0.637	5.736	4.371	4.417	2.197	2.239
$\Sigma$	6.780	7.013	7.429	7.852	7.598	7.736	7.751	7.761	7.568	7.675	7.949	7.962	7.895	7.730	7.829
S	12.108	12.236	11.980	12.051	12.053	12.110	12.165	11.917	12.519	12.448	12.252	12.007	12.137	12.481	12.495
Se	0.048	0.047	0.057	0.051	0.056	0.000	0.082	0.065	0.038	0.025	0.000	0.000	0.000	0.000	0.000
$\Sigma$	12.156	12.283	12.037	12.103	12.109	12.110	12.247	11.982	12.557	12.473	12.252	12.007	12.137	12.481	12.495
Cl	0.000	0.000	0.000	0.000	0.000	0.000	0.068	0.000	0.000	0.000	0.000	0.000	0.000	0.000	0.000
$n_{\text{aik}}$	30.5	24.7	14.3	3.7	10.0	6.6	6.2	6.0	10.8	8.1	1.3	1.0	2.6	6.8	4.3

calculated empirical formulae are based on  $(\text{Cu} + \text{Pb})/2 + (\text{Sb} + \text{Bi}) = 8 \text{ apfu}$

h.r. – host rock; LG – leucogranite; PG – porphyric granite

## 4. Results and discussion

### 4.1. Bismuthinite-aikinite series

Minerals of the bismuthinite-aikinite series, represented predominantly by bismuthinite are common, both in quartz veins hosted in porphyric granite as well as in P-enriched leucogranites. They form metallic lead grey to steel grey, prismatic to acicular crystals up to 1.5 cm, or irregular aggregates up to  $2 \times 2$  cm in size enclosed in quartz. Bismuthinite is only very rarely directly associated with other sulfosalts (kobellite, Fig. 2a, 2b), but it is often accompanied by native bismuth, pyrite, fluorite,

fluorapatite, triplite, polycrase-(Y), Li-bearing micas or siderite.

Representative WDS analyses of minerals of the bismuthinite-aikinite series are given in Tab. 1 (all

131 analyses and corresponding calculated empirical formulae are available in the supplementary data). Makovicky and Makovicky (1978) proposed to characterize members of the bismuthinite-aikinite series by

$n_{\text{aik}}$ , which corresponds to the percentage of  $\text{CuPbBiS}_3$  end-member in the  $\text{Bi}_2\text{S}_3\text{-CuPbBiS}_3$  series. Based on this approach, the vast majority of samples from Gemerská Poloma correspond to bismuthinite (Fig. 3a), with the calculated value of  $n_{\text{aik}}$  ranging between 1.0 to 14.3 (containing up to 0.58 *apfu* of Cu and 0.57 *apfu* of Pb). In one sample, exsolved lamellae, and ribbons hosted in bismuthinite were observed (Fig. 2a, 2b). These phases with  $n_{\text{aik}}$  ranging from 21.3 to 23.7 and 30.3 (Fig. 3a) are fitting to the compositional gap between pekoite (with  $n_{\text{aik}} = 16.7$ ) and gladite ( $n_{\text{aik}} = 33.3$ ) and may represent new members of the bismuthinite-aikinite series. Similar exsolved phases with  $n_{\text{aik}} = 21\text{--}22$  and  $n_{\text{aik}} = 25\text{--}27$  were described by Topa et al. (2002) from Felbertal scheelite deposit (Austria), as well as by Cook (1997) from epithermal veins near Baia Borsă (Romania), Ciobanu and Cook (2000) and Cook and Ciobanu (2003) from Ocna de Fier skarn deposit (Romania), Xiang-Ping et al. (2001) from Funishan skarn deposit (China), Pršek and Mikuš (2006) from Kolba deposit near Lúbietová (Slovakia) or Voudouris et al. (2013) from Stanos deposit in Chalkidiki (Greece). The amount of Sb substituting for Bi (Fig. 3b) varies in the studied samples considerably from 0.55 up to

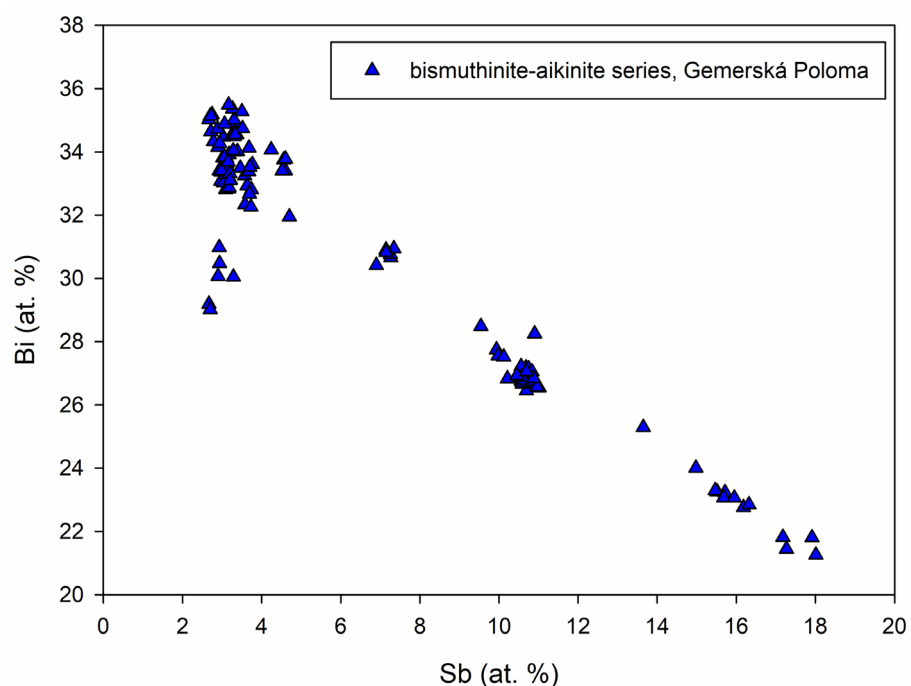
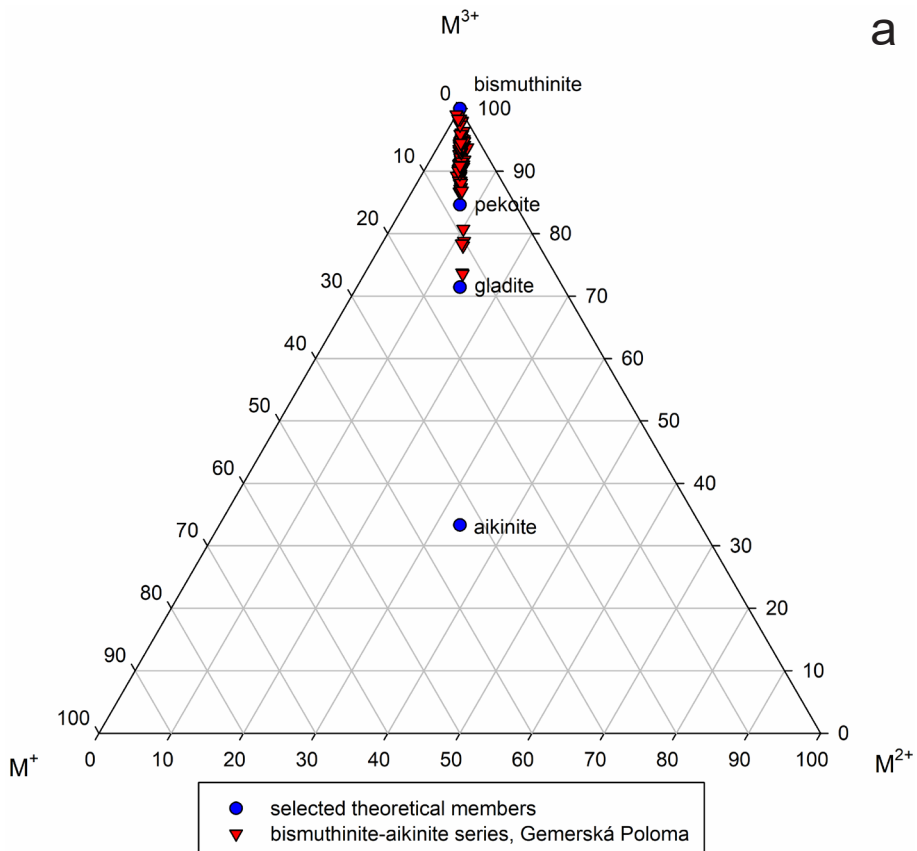


**Fig. 3a** – The composition of minerals of the bismuthinite-aikinite series from Gemerská Poloma in ternary plot  $M^+ - M^{2+} - M^{3+}$ . **b** – Variation of Sb and Bi contents (at. %) in minerals of the bismuthinite-aikinite series from Gemerská Poloma.

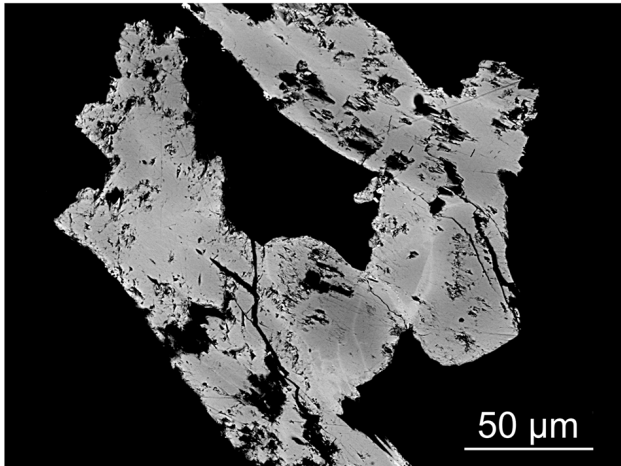
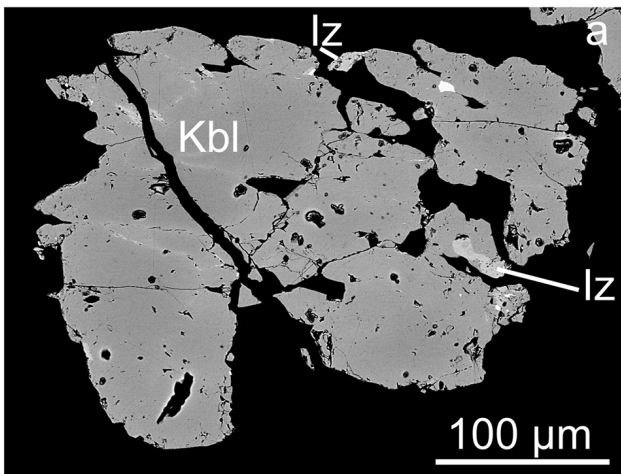


**Fig. 4** Irregular chemical zoning of bismuthinite caused by variation of Bi and Sb contents. Sample GPA2, BSE image.

3.63 *apfu*, locally causing weak, irregular chemical zoning (Fig. 4). The samples from quartz veins hosted in porphyric granite tend to be more Sb enriched than those from P-enriched leucogranites. Besides, minor concentrations of Se (up to 0.09 *apfu*) were also detected in some samples.



#### 4.2. Kobellite homologous series

##### 4.2.1. Kobellite–tintinaite series

Minerals of the kobellite–tintinaite series are the most common sulfosalts and occur as individual acicular to prismatic crystals up to 1.5 cm or radial groups and irregular aggregates up to  $3 \times 3$  cm in size embedded in quartz. They occur both in porphyric as well as in P-enriched leucogranites and are associated with bismuthinite (Fig. 2a, 2b), minerals of the giessenite–izoklakeite series (Fig. 5a), tiny inclusions of native bismuth and locally also with jamesonite (Fig. 5b), galena or bournonite. Other minerals frequently associated with minerals of the kobellite–tintinaite series are pyrite, fluorite, fluorapatite, siderite and albite.

Representative chemical analyses of minerals of the kobellite–tintinaite series from Gemerská Poloma and the corresponding empirical formulae are shown in Tab. 2 (all 208 analyses and calculated empirical formulae are available in supplementary data). The calculated value of *N* (order number of kobellite homolog, see Zakrzewski and Makovicky 1986 for details) ranges from 1.85 to

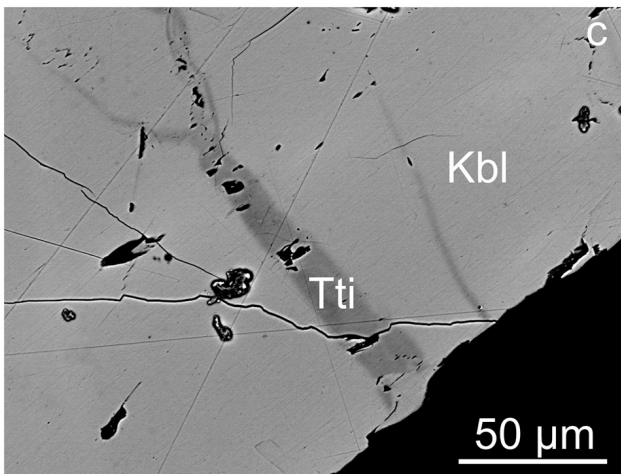
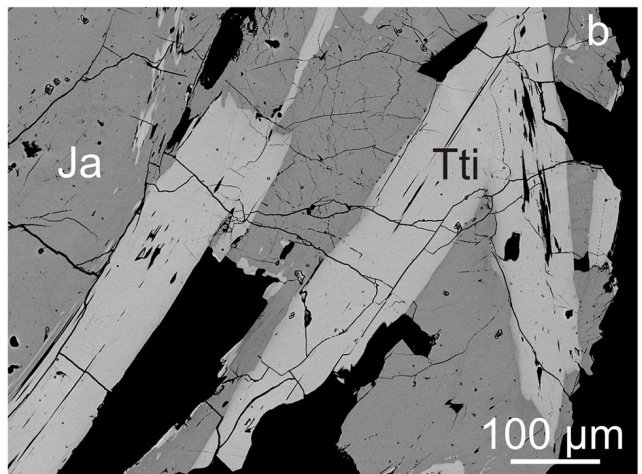


**Fig. 5a** – Kobellite (Kbl) associated with tiny inclusions of minerals of the giessenite–izoklakeite series (Iz) and galena (white). Sample GPES4, BSE image. **b** – Tintinaite (Tti) associated with jamesonite (Ja). Sample GPES5, BSE image. **c** – Irregular veinlets of tintinaite (Tti) developed in kobellite (Kbl). Sample GPES4, BSE image.

**Tab. 2** Representative chemical analyses of minerals of the kobellite–tintinaite series from Gemerská Poloma (in wt. %)

h.r.	GPES1		GPES2		GPES4		GPES5		GPX2		GPA1		GPA2	GPA5	GPA7
	LG		LG		LG		PG		PG		PG		PG	PG	LG
	Kbl	Kbl	Kbl	Tti	Kbl	Tti	Kbl								
Pb	32.66	32.37	32.76	30.77	33.19	36.37	34.40	34.67	34.58	34.57	36.62	36.11	34.27	37.01	34.43
Ag	0.26	0.29	0.22	0.00	0.22	0.00	0.19	0.13	0.13	0.00	0.12	0.16	0.48	0.00	0.00
Cu	1.70	1.75	1.76	1.65	1.64	1.83	2.28	2.13	2.09	2.15	2.01	2.00	1.84	1.88	1.64
Fe	0.26	0.29	0.20	0.00	0.29	0.31	0.00	0.00	0.00	0.05	0.18	0.21	0.26	0.27	0.26
Zn	0.00	0.00	0.00	0.00	0.00	0.00	0.00	0.00	0.00	0.00	0.00	0.10	0.00	0.00	0.09
Sb	7.85	8.82	9.37	4.64	9.31	17.88	22.40	24.18	20.27	22.92	23.45	23.58	18.97	21.70	11.09
Bi	38.84	38.44	37.43	44.95	37.04	24.86	20.61	19.50	23.24	20.24	17.89	17.60	24.81	19.56	34.30
S	18.21	18.29	17.61	17.15	18.21	19.21	19.79	19.24	19.99	20.18	19.92	19.72	19.48	19.71	18.55
Se	0.00	0.00	0.20	0.32	0.00	0.00	0.00	0.00	0.00	0.00	0.00	0.00	0.00	0.00	0.00
Cl	0.00	0.07	0.00	0.05	0.09	0.11	0.00	0.00	0.00	0.00	0.06	0.00	0.00	0.00	0.00
total	99.78	100.32	99.55	99.53	99.99	100.57	99.67	99.85	100.30	100.10	100.25	99.48	100.11	100.13	100.36
Pb	9.835	9.646	9.969	9.665	9.919	10.260	9.479	9.637	9.540	9.419	9.997	9.933	9.598	10.234	10.147
Ag	0.150	0.166	0.129	0.000	0.126	0.000	0.101	0.070	0.068	0.000	0.063	0.085	0.256	0.000	0.000
$\Sigma$	9.986	9.812	10.097	9.665	10.046	10.260	9.580	9.707	9.607	9.419	10.060	10.017	9.855	10.234	10.147
Cu	1.669	1.700	1.746	1.690	1.598	1.683	2.049	1.930	1.881	1.910	1.789	1.794	1.684	1.694	1.576
Fe	0.291	0.321	0.226	0.000	0.322	0.324	0.000	0.000	0.000	0.050	0.182	0.214	0.274	0.280	0.284
Zn	0.000	0.000	0.000	0.000	0.000	0.000	0.000	0.000	0.000	0.000	0.087	0.000	0.000	0.000	0.084
$\Sigma$	1.960	2.021	1.972	1.690	1.920	2.008	2.049	1.930	1.881	1.960	1.971	2.095	1.957	1.974	1.944
Sb	4.023	4.472	4.852	2.480	4.735	8.583	10.504	11.439	9.515	10.627	10.893	11.037	9.043	10.215	5.562
Bi	11.597	11.357	11.293	13.999	10.976	6.953	5.631	5.374	6.359	5.467	4.842	4.800	6.889	5.364	10.022
$\Sigma$	15.620	15.829	16.145	16.480	15.711	15.536	16.135	16.813	15.874	16.095	15.736	15.837	15.933	15.579	15.584
S	35.435	35.216	34.626	34.810	35.167	35.015	35.237	34.550	35.638	35.527	35.138	35.050	35.255	35.213	35.325
Se	0.000	0.000	0.160	0.264	0.000	0.000	0.000	0.000	0.000	0.000	0.000	0.000	0.000	0.000	0.000
$\Sigma$	35.435	35.216	34.786	35.073	35.167	35.015	35.237	34.550	35.638	35.527	35.138	35.050	35.255	35.213	35.325
Cl	0.000	0.122	0.000	0.092	0.157	0.181	0.000	0.000	0.000	0.000	0.096	0.000	0.000	0.000	0.000
N	2.00	1.95	1.98	1.91	1.98	2.00	1.95	1.90	1.97	1.89	2.00	2.00	1.98	2.01	2.00

calculated empirical formulae are based on sum of all atoms = 63 *apfu*  
 h.r. – host rock; LG – leucogranite; PG – porphyric granite

2.06. The Sb/(Sb+Bi) atomic ratio in samples from Gemerská Poloma (Fig. 6) varies considerably between 0.13

and 0.71, representing a rather wide compositional range between kobellite and tintinaite. However, in individual samples, the Sb *versus* Bi variation tends to be relatively small and only weak chemical zoning was rarely observed in one case (Fig. 5c, sample GPES4). In general, samples from the quartz veins hosted in porphyric granite tend to be Sb-dominant (tintinaite), whereas Bi-dominant compositions (kobellite) prevail in quartz veins hosted in P-enriched leucogranite. All studied samples contain significant concentrations of Cu (1.44 up to 2.05 *apfu*), but variable amounts of Fe (0.00 up to 0.61 *apfu*). Variation of Cu and Fe contents in minerals of the kobellite-tintinaite series from Gemerská Poloma is shown in Fig. 7a. The overall Cu+Fe content ranges from

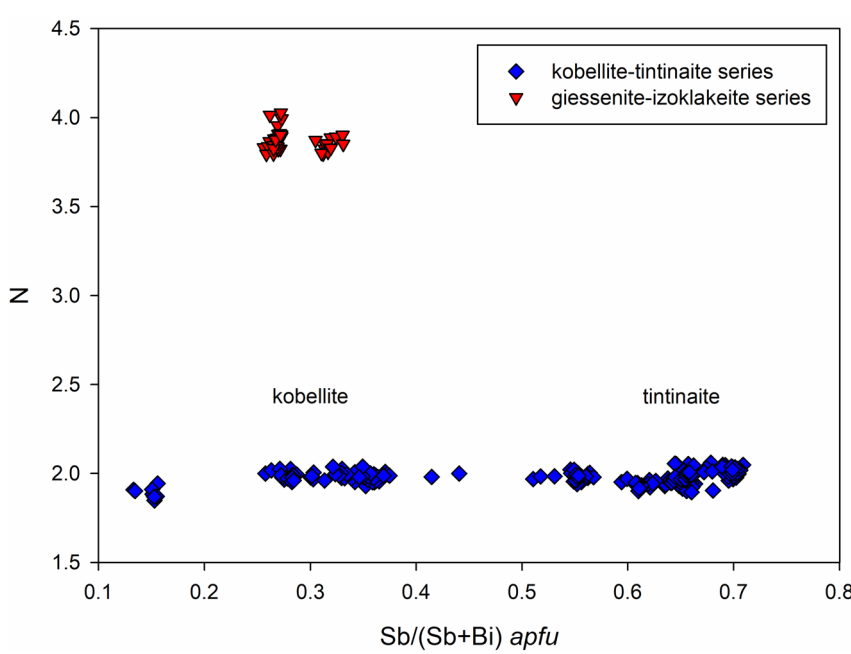


**Fig. 6** Variation of Sb/(Sb+Bi) ratio and calculated value of N for minerals of the kobellite homologous series from Gemerská Poloma.

1.65 to 2.10  $\text{apfu}$ , with an average of 1.95  $\text{apfu}$ , close to the ideal value of 2  $\text{apfu}$  (e.g., Zakrzewski and Makovicky 1986; Moëlo et al. 1995; Wagner and Johnsson 2001; Pršek et al. 2008; Mikuš et al. 2018). The maximum content of Ag substituting for Pb (Fig. 7b) is 0.26  $\text{apfu}$ . In addition, minor amounts of Zn (up to 0.09  $\text{apfu}$ ), Se (up to 0.26  $\text{apfu}$ ) and Cl (up to 0.40  $\text{apfu}$ ) were also locally detected.

#### 4.2.2. Giessenite–izoklakeite series

Minerals of the giessenite–izoklakeite series are rare and were identified only in two samples, both from the quartz veins hosted in P-enriched leucogranite. They form subhedral grains and aggregates reaching up to 100  $\mu\text{m}$  in size intimately intergrown with kobellite (Fig. 5a, 8). Representative chemical analyses of minerals of the giessenite–izoklakeite series from Gemerská Poloma and the corresponding empirical formulae are given in Tab. 3 (all 45 analyses and calculated empirical formulae are available in supplementary data). The calculated values of  $N$  range from 3.80 to 4.03. The values of  $\text{Sb}/(\text{Sb} + \text{Bi})$  ratio in studied samples vary from 0.26 to 0.33 (Fig. 6) and slightly differ between the two studied samples (0.26 to 0.27 in sample GPES4 and 0.31 to 0.33 in sample GPA7).

There is only a quasi-continuous solid solution between giessenite and izoklakeite with increasing  $\text{Sb}/\text{Bi}$  ratio (Moëlo et al. 2008) since, according to the published data, the symmetry of giessenite is monoclinic (Graser and Harris 1986; Makovicky and Karup-Møller 1986) and that of Bi-rich izoklakeite is orthorhombic (Harris et al. 1986; Makovicky and Mumme 1986; Armbruster and Hummel 1987). The exact  $\text{Sb}/\text{Bi}$  ratio at which the symmetry changes is unknown, but according to Moëlo et al. (1995, 2008), the name izoklakeite is applied to all phases with  $\text{Sb}/\text{Bi}$  atomic ratio close to 1 (i.e.,  $\text{Sb}/(\text{Sb} + \text{Bi})$  close to 0.50), even for samples with  $\text{Bi} > \text{Sb}$ . Pažout

et al. (2017) estimated that the symmetry change between giessenite and izoklakeite takes place somewhere in the range of  $\text{Sb}/(\text{Sb} + \text{Bi})$  values of 0.20 to 0.30. Ozawa et al. (1998) described so far the most Bi-enriched izoklakeite from Otome mine in Japan with  $\text{Sb}/(\text{Sb} + \text{Bi})$  ratio ranging from 0.31 to 0.33. Thus, it is possible that both giessenite and Bi-rich izoklakeite are present at Gemerská Poloma, but all attempts to extract suitable single-crystals to confirm this hypothesis by single-crystal XRD were unsuccessful. Both studied samples of minerals of the giessenite–izoklakeite series contain substantial amounts of Cu (1.81 to 2.15  $\text{apfu}$ ), but surprisingly no Fe (Fig. 7a). Furthermore, the

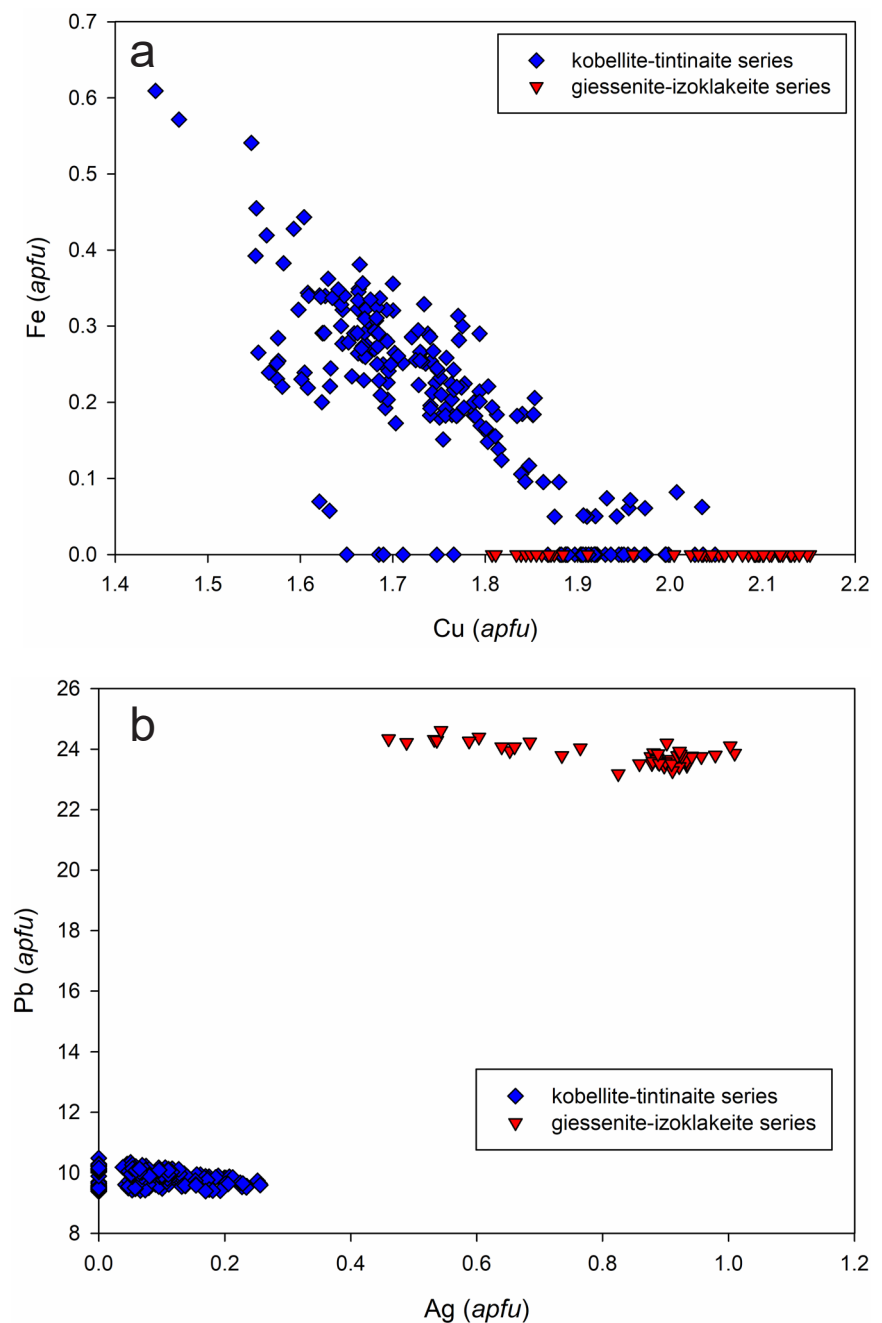


**Fig. 7a** – Cu vs. Fe ( $\text{apfu}$ ) plot for members of the kobellite homologous series from Gemerská Poloma. **b** – Ag vs. Pb ( $\text{apfu}$ ) plot for members of the kobellite homologous series from Gemerská Poloma.

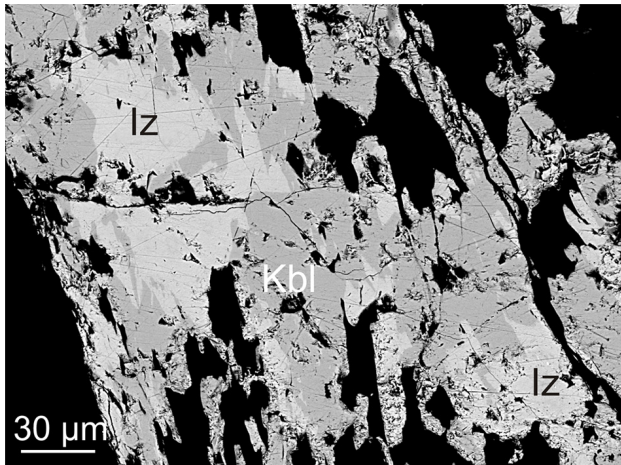


**Fig. 8** Minerals of the giessenite-izoklakite series (Iz) intergrown with kobellite (Kbl). Sample GPA7, BSE image.

**Tab. 3** Representative chemical analyses of minerals of the giessenite–izoklakite series from Gemerská Poloma (in wt. %)

	GPES4							GPA7							
Pb	45.11	44.76	44.42	44.31	44.94	44.82	45.86	46.51	46.65	46.76	46.23	46.59	47.01	46.27	45.98
Ag	0.93	0.86	0.91	0.82	0.99	0.85	0.89	0.53	0.49	0.46	0.66	0.60	0.54	0.64	0.74
Cu	1.19	1.19	1.14	1.19	1.23	1.26	1.24	1.06	1.07	1.11	1.08	1.08	1.09	1.09	1.10
Sb	6.43	6.02	6.10	6.04	6.33	6.25	6.08	7.34	7.33	7.41	7.38	7.13	7.45	7.41	7.58
Bi	29.40	30.00	29.79	29.72	28.92	29.67	29.41	27.56	27.72	27.43	28.12	27.90	27.27	27.54	27.72
S	16.97	16.65	16.92	17.20	16.63	16.89	16.69	17.02	17.21	17.12	17.05	16.94	16.90	17.15	17.27
Cl	0.00	0.00	0.00	0.00	0.00	0.06	0.00	0.00	0.00	0.00	0.00	0.00	0.00	0.00	0.00
total	100.03	99.48	99.28	99.27	99.04	99.80	100.17	100.02	100.47	100.29	100.52	100.24	100.26	100.10	100.39
Pb	23.623	23.752	23.422	23.188	23.861	23.516	24.200	24.323	24.220	24.343	24.075	24.396	24.616	24.077	23.787
Ag	0.933	0.877	0.922	0.825	1.010	0.858	0.902	0.532	0.489	0.460	0.660	0.603	0.543	0.640	0.735
$\Sigma$	24.556	24.629	24.344	24.013	24.871	24.375	25.101	24.856	24.708	24.803	24.735	25.000	25.160	24.716	24.522
Cu	2.039	2.059	1.960	2.022	2.129	2.151	2.140	1.808	1.811	1.884	1.834	1.844	1.861	1.849	1.856
Sb	5.726	5.436	5.473	5.377	5.719	5.577	5.456	6.532	6.476	6.565	6.540	6.353	6.639	6.561	6.673
Bi	15.262	15.784	15.574	15.422	15.225	15.435	15.387	14.290	14.269	14.158	14.519	14.485	14.158	14.208	14.218
$\Sigma$	20.989	21.220	21.047	20.798	20.944	21.012	20.844	20.822	20.745	20.723	21.059	20.838	20.797	20.770	20.891
S	57.416	57.092	57.649	58.166	57.056	57.275	56.915	57.515	57.735	57.590	57.373	57.318	57.183	57.664	57.731
Cl	0.000	0.000	0.000	0.000	0.000	0.187	0.000	0.000	0.000	0.000	0.000	0.000	0.000	0.000	0.000
N	3.89	3.83	3.84	3.80	3.99	3.83	4.01	3.82	3.80	3.81	3.80	3.87	3.89	3.85	3.83

calculated empirical formulae are based on sum of all atoms = 105 *apfu*

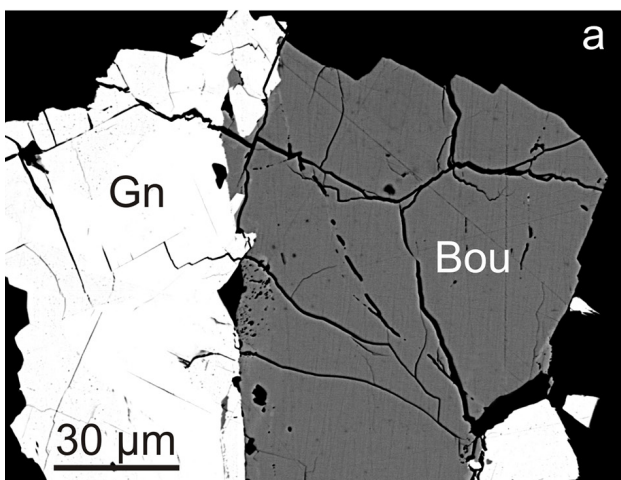


**Fig. 9a** – Boulangerite (Bou) in contact with galena (Gn). Sample GPN4, BSE image. **b** – Boulangerite (Bou) associated with jamesonite (Ja) and galena (white). Sample GPN7, BSE image.

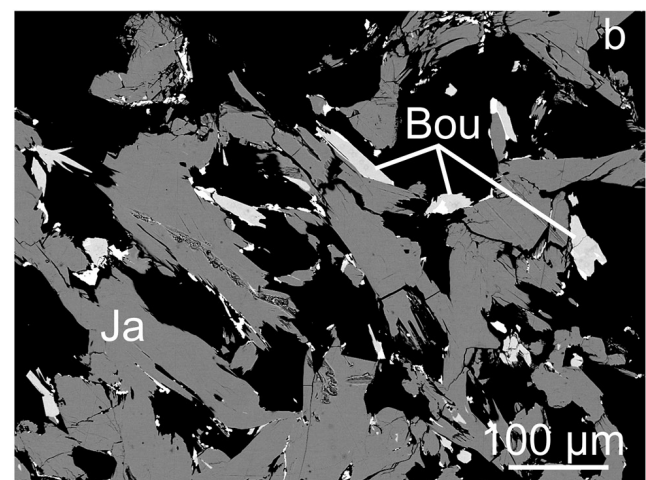
presence of Ag (ranging from 0.46 to 1.01 *apfu*) substituting for Pb (Fig. 7b) according to lillianite type substitution  $\text{Ag}+\text{Bi}=2\text{Pb}$  is typical.

#### 4.3. Pb–Sb sulfosalts

Pb–Sb sulfosalts, especially jamesonite and robinsonite, as well as minor amounts of boulangerite are common minerals in quartz veins hosted in porphyric granite, but they are absent in hydrothermal quartz veins hosted in P-enriched leucogranite.

##### 4.3.1. Boulangerite

Boulangerite is infrequent. It occurs as acicular crystals up to 7 mm long, developed together with jamesonite in



**Tab. 4** Representative chemical analyses of boulangerite from Gemerská Poloma (in wt. %)

	GPX3		GPN1			GPN2		GPN3			GPN5		GPN6		
Pb	38.59	38.33	39.68	39.98	38.93	39.71	39.88	37.53	39.54	38.36	40.52	40.35	41.28	41.40	40.56
Cu	0.00	0.00	0.00	0.00	0.00	0.00	0.00	0.00	0.07	0.00	0.00	0.10	0.00	0.00	0.00
Fe	0.00	0.00	0.00	0.00	0.00	0.00	0.00	0.00	0.00	0.00	0.00	0.00	0.00	0.11	0.00
Sb	25.37	25.31	30.22	31.27	28.48	30.81	31.83	22.14	30.05	25.98	33.43	32.39	36.75	35.56	34.36
Bi	15.90	16.05	9.48	8.45	12.66	9.29	7.77	20.33	10.68	15.30	5.88	6.77	1.34	3.00	4.27
S	20.12	20.11	20.70	20.99	20.81	20.96	20.63	19.72	20.30	19.92	20.24	20.47	20.46	20.13	20.47
Cl	0.00	0.00	0.05	0.00	0.00	0.00	0.00	0.00	0.00	0.00	0.00	0.07	0.00	0.00	0.00
total	99.98	99.79	100.13	100.69	100.88	100.77	100.12	99.72	100.64	99.63	100.07	100.09	99.83	100.20	99.66
Pb	3.901	3.879	3.892	3.877	3.820	3.857	3.902	3.874	3.909	3.889	3.982	3.953	4.000	4.046	3.961
Cu	0.000	0.000	0.000	0.000	0.000	0.000	0.000	0.000	0.023	0.000	0.000	0.031	0.000	0.000	0.000
Fe	0.000	0.000	0.000	0.000	0.000	0.000	0.000	0.000	0.000	0.000	0.000	0.000	0.000	0.040	0.000
$\Sigma$	3.901	3.879	3.892	3.877	3.820	3.857	3.902	3.874	3.931	3.889	3.982	3.984	4.000	4.085	3.961
Sb	4.364	4.359	5.042	5.160	4.755	5.093	5.300	3.890	5.055	4.482	5.591	5.400	6.060	5.913	5.710
Bi	1.594	1.611	0.922	0.812	1.232	0.895	0.754	2.081	1.047	1.538	0.573	0.657	0.129	0.291	0.413
$\Sigma$	5.958	5.970	5.964	5.972	5.987	5.987	6.054	5.971	6.102	6.020	6.164	6.057	6.189	6.204	6.123
S	13.141	13.151	13.116	13.151	13.194	13.155	13.043	13.155	12.967	13.049	12.854	12.958	12.811	12.711	12.916
Cl	0.000	0.000	0.028	0.000	0.000	0.000	0.000	0.000	0.000	0.041	0.000	0.000	0.000	0.000	0.000

are based on sum of all atoms = 23 *apfu*

cavities of quartz, subhedral to anhedral grains and aggregates replacing galena (Fig. 9a, GPN4) or individual subhedral crystals up to 100 µm in size associated with jamesonite (Fig. 9b, GPN7). Other accompanying minerals are sphalerite, pyrite, fluorite, siderite, dolomite and albite. Representative chemical analyses of boulangerite are shown in Tab. 4 (all 61 analyses and calculated empirical formulae are available in supplementary data). Elevated contents of Bi (up to 0.32 *apfu*) substituting for Sb are typical (Fig. 10). Minor amounts of other elements such as Fe, As or Cl (all reaching up to 0.04 *apfu*) were also detected.

#### 4.3.2. Robinsonite

Robinsonite is a common sulfosalt in quartz veins hosted in porphyric granite. It forms irregular or radial aggregates up to 3 × 3 cm in size, consisting of individual acicular crystals up to 1.5 cm long. Groups and aggregates of acicular crystals of robinsonite included in fluorite were also observed. Robinsonite is frequently associated mainly with jamesonite (Fig. 11), galena or sphalerite.

Quantitative chemical analyses and the corresponding calculated empirical formulae of

robinsonite from Gemerská Poloma are given in Tab. 5 (all 107 analyses and calculated empirical formulae are available in supplementary data). Significant incorporation of Bi (ranging from 0.13 up to 2.08 *apfu*) is characteristic for robinsonite from Gemerská Poloma (Fig. 10). Similar elevated contents of Bi in robinsonite were so far described only by Jambor and Lachance (1968) from the Dodger tungsten mine in British Columbia (Canada), or by Števko and Sejkora (2017) from Čížko baňa occurrence near Ochtiná (Slovakia). Furthermore, minor concentrations of Fe (up to 0.07 *apfu*), Cu (up to 0.03 *apfu*) as well as Cl (up to 0.04 *apfu*) are present in robinsonite.

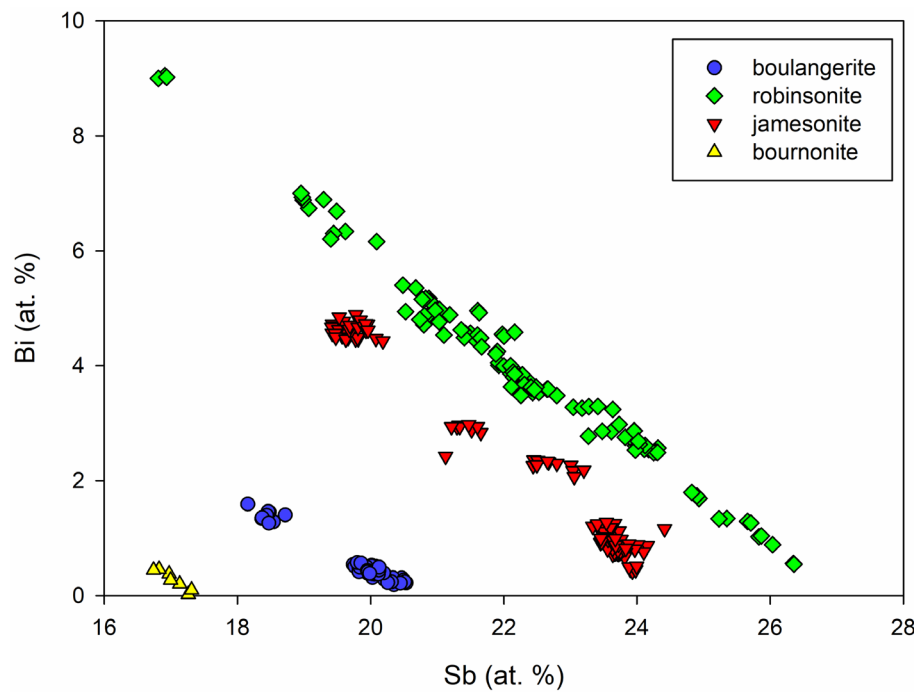


**Fig. 10** Variation of Sb and Bi contents (at. %) in Pb–Sb sulfosalts and bournonite from Gemerská Poloma.

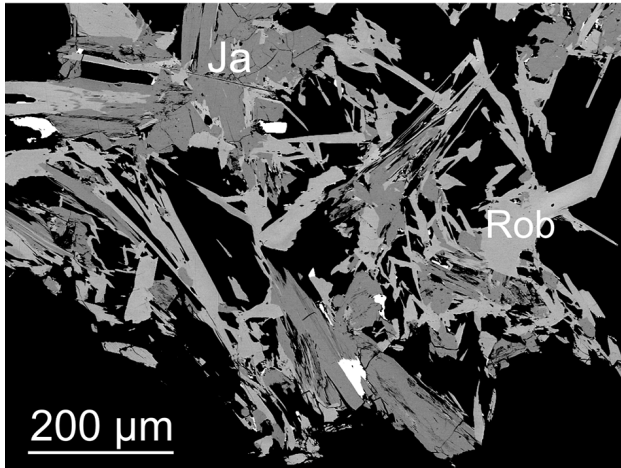


**Fig. 11** Crystals of robinsonite (Rob) associated with jamesonite (Ja) and galena (white). Sample GPN5, BSE image.

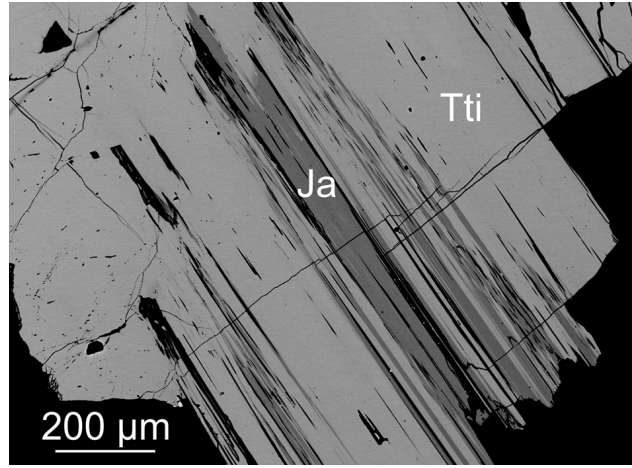


**Fig. 12** Crystals of jamesonite (Ja) enclosed in tintinaite (Tti). Sample GPX2, BSE image.

#### 4.3.3. Jamesonite

Jamesonite is an abundant mineral and it occurs as radial or irregular aggregates up to 3 cm embedded in quartz, which consists of individual acicular crystals up to 1 cm long. It is predominantly associated with other Pb–Sb sulfosalts (robinsonite, boulangerite; Fig. 9b, 11) as well as sphalerite, galena, pyrite, arsenopyrite, fluorite, siderite and dolomite. In two cases, minerals of the kobellite–tintinaite series (tintinaite; Fig. 12) were also found in direct association with jamesonite.

Representative chemical analyses of jamesonite from Gemerská Poloma and the corresponding empirical formulae are given in Tab. 6 (all 128 analyses and calculated empirical formulae are available in supplementary data). Jamesonite is characterized especially by an elevated content of Bi (ranging from 0.11 up to 1.22 *apfu*) substi-

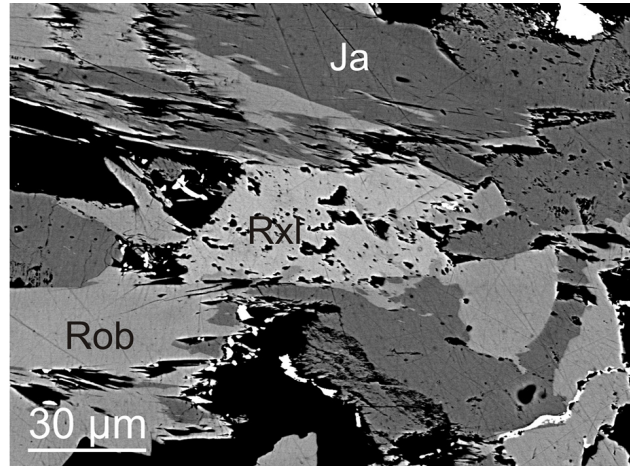


**Fig. 13** Rouxelite (Rxl) associated with robinsonite (Rob), jamesonite (Ja) and galena (white). Sample GPN5, BSE image.

**Tab. 5** Representative chemical analyses of robinsonite from Gemerská Poloma (in wt. %)

	GPX3		GPN1		GPN2		GPN3		GPN5		GPN6	
Pb	38.59	38.33	39.68	39.98	38.93	39.71	39.88	37.53	39.54	38.36	40.52	40.35
Cu	0.00	0.00	0.00	0.00	0.00	0.00	0.00	0.00	0.07	0.00	0.00	0.10
Fe	0.00	0.00	0.00	0.00	0.00	0.00	0.00	0.00	0.00	0.00	0.00	0.11
Sb	25.37	25.31	30.22	31.27	28.48	30.81	31.83	22.14	30.05	25.98	33.43	32.39
Bi	15.90	16.05	9.48	8.45	12.66	9.29	7.77	20.33	10.68	15.30	5.88	6.77
S	20.12	20.11	20.70	20.99	20.81	20.96	20.63	19.72	20.30	19.92	20.24	20.47
Cl	0.00	0.00	0.05	0.00	0.00	0.00	0.00	0.00	0.00	0.07	0.00	0.00
total	99.98	99.79	100.13	100.69	100.88	100.77	100.12	99.72	100.64	99.63	100.07	100.09
Pb	3.901	3.879	3.892	3.877	3.820	3.857	3.902	3.874	3.909	3.889	3.982	3.953
Cu	0.000	0.000	0.000	0.000	0.000	0.000	0.000	0.000	0.023	0.000	0.000	0.031
Fe	0.000	0.000	0.000	0.000	0.000	0.000	0.000	0.000	0.000	0.000	0.000	0.040
Σ	3.901	3.879	3.892	3.877	3.820	3.857	3.902	3.874	3.931	3.889	3.982	3.984
Sb	4.364	4.359	5.042	5.160	4.755	5.093	5.300	3.890	5.055	4.482	5.591	5.400
Bi	1.594	1.611	0.922	0.812	1.232	0.895	0.754	2.081	1.047	1.538	0.573	0.657
Σ	5.968	5.970	5.964	5.972	5.987	5.988	6.054	5.971	6.102	6.020	6.164	6.057
S	13.141	13.151	13.116	13.151	13.194	13.155	13.043	13.155	12.967	13.049	12.854	12.958
Cl	0.000	0.000	0.028	0.000	0.000	0.000	0.000	0.000	0.000	0.041	0.000	0.000

calculated empirical formulae are based on sum of all atoms = 23 *apfu*

**Tab. 6** Representative chemical analyses of jamesonite from Gemerská Poloma (in wt. %)

	GPES5	GPES9	GPX2	GPX3	GPN2		GPN5		GPN6		GPN7	GPN8	GPA3		GPA4
Pb	37.20	38.86	36.82	37.71	37.85	37.92	38.09	38.75	39.22	39.71	39.02	39.06	38.37	38.76	38.47
Cu	0.14	0.09	0.31	0.17	0.07	0.07	0.11	0.16	0.06	0.00	0.00	0.00	0.02	0.00	0.12
Fe	2.30	2.42	2.07	2.24	2.33	2.32	2.34	2.24	2.46	2.49	2.52	2.53	2.56	2.52	2.39
Zn	0.00	0.00	0.00	0.00	0.08	0.11	0.07	0.00	0.00	0.00	0.00	0.00	0.00	0.00	0.00
Cd	0.00	0.00	0.00	0.00	0.00	0.00	0.11	0.17	0.00	0.00	0.00	0.00	0.00	0.00	0.00
Sb	27.85	30.80	27.63	28.06	31.18	31.13	32.29	32.90	34.84	35.24	34.96	34.14	35.38	35.55	34.94
Bi	11.82	6.07	11.54	11.34	7.01	7.40	5.82	5.07	2.20	1.90	1.69	3.17	1.16	1.31	2.51
S	20.79	21.91	21.37	21.18	21.37	21.56	21.12	20.72	21.18	21.36	21.71	21.22	22.07	22.01	21.89
Cl	0.00	0.00	0.00	0.05	0.00	0.00	0.00	0.00	0.00	0.00	0.00	0.00	0.00	0.00	0.00
total	100.10	100.14	99.75	100.74	99.89	100.51	99.96	100.01	99.96	100.70	99.90	100.11	99.55	100.15	100.32
Pb	3.881	3.916	3.802	3.885	3.861	3.842	3.890	3.990	3.971	3.990	3.905	3.957	3.808	3.843	3.830
Cu	0.048	0.029	0.105	0.058	0.023	0.023	0.037	0.054	0.020	0.000	0.000	0.000	0.007	0.000	0.039
Fe	0.890	0.904	0.795	0.854	0.882	0.872	0.887	0.857	0.924	0.928	0.936	0.949	0.941	0.927	0.884
Zn	0.000	0.000	0.000	0.000	0.026	0.035	0.023	0.000	0.000	0.000	0.000	0.000	0.000	0.000	0.000
Cd	0.000	0.000	0.000	0.000	0.000	0.000	0.021	0.033	0.000	0.000	0.000	0.000	0.000	0.000	0.000
$\Sigma$	4.819	4.850	4.703	4.797	4.791	4.773	4.858	4.935	4.915	4.918	4.840	4.906	4.756	4.770	4.754
Sb	4.944	5.281	4.856	4.920	5.413	5.368	5.613	5.765	6.003	6.025	5.953	5.885	5.975	5.999	5.919
Bi	1.223	0.606	1.181	1.158	0.709	0.743	0.590	0.517	0.221	0.189	0.168	0.319	0.114	0.128	0.248
$\Sigma$	6.167	5.887	6.037	6.078	6.122	6.111	6.203	6.282	6.224	6.214	6.121	6.204	6.089	6.127	6.167
S	14.015	14.263	14.260	14.096	14.087	14.116	13.939	13.783	13.861	13.867	14.038	13.891	14.155	14.103	14.080
Cl	0.000	0.000	0.000	0.029	0.000	0.000	0.000	0.000	0.000	0.000	0.000	0.000	0.000	0.000	0.000

calculated empirical formulae are based on sum of all atoms = 25 *apfu*

tuting for Sb (Fig. 10). Pažout (2020) recently solved the crystal structure of Bi-rich jamesonite from Kutná Hora and confirmed that Bi content is distributed over all three sites occupied by Sb without any preferential placement of Bi into one of the three Sb sites. Other minor elements detected in jamesonite are Cu (up to 0.11 *apfu*), Zn (up to 0.04 *apfu*), Cd (up to 0.03 *apfu*) and locally also Cl (up to 0.03 *apfu*).

**Tab. 7** Chemical composition of rouxelite from Gemerská Poloma (in wt. %)

	GPN5											
Pb	43.46	43.94	43.50	43.86	44.00	43.79	44.27	44.31	44.12	44.31	43.86	43.30
Ag	0.14	0.19	0.14	0.16	0.20	0.17	0.17	0.21	0.17	0.16	0.19	0.22
Hg	1.11	1.37	1.48	1.25	1.29	1.25	1.26	1.40	1.33	1.34	1.31	1.33
Cu	1.16	1.17	1.17	1.16	1.15	1.17	1.18	1.16	1.18	1.15	1.12	1.18
Fe	0.06	0.00	0.00	0.00	0.06	0.00	0.06	0.00	0.05	0.00	0.00	0.00
Sb	27.67	27.83	27.64	27.73	28.69	28.31	28.61	28.40	28.56	27.94	28.26	27.57
Bi	6.16	6.27	6.30	6.33	5.31	5.97	5.31	5.23	5.37	5.64	5.84	6.24
S	19.79	19.56	19.65	19.71	19.48	19.81	19.76	19.49	19.44	19.64	19.60	19.80
total	99.55	100.33	99.88	100.20	100.18	100.47	100.62	100.19	100.22	100.18	100.17	99.64
Cu	1.964	1.961	1.975	1.952	1.915	1.959	1.962	1.940	1.965	1.934	1.881	1.998
Fe	0.116	0.000	0.000	0.000	0.114	0.000	0.114	0.000	0.095	0.000	0.000	0.000
$\Sigma$	2.079	1.961	1.975	1.952	2.029	1.959	2.076	1.940	2.060	1.934	1.881	1.998
Hg	0.595	0.727	0.791	0.666	0.681	0.662	0.664	0.740	0.702	0.712	0.695	0.714
Ag	0.140	0.188	0.139	0.159	0.196	0.165	0.167	0.203	0.167	0.156	0.185	0.219
$\Sigma$	0.735	0.915	0.930	0.825	0.877	0.827	0.830	0.943	0.868	0.868	0.880	0.933
Pb	22.566	22.586	22.516	22.633	22.472	22.464	22.578	22.703	22.532	22.824	22.546	22.489
Sb	24.449	24.343	24.346	24.351	24.934	24.711	24.830	24.758	24.821	24.493	24.719	24.367
Bi	3.171	3.195	3.233	3.239	2.689	3.039	2.685	2.655	2.719	2.880	2.975	3.213
$\Sigma$	27.620	27.538	27.579	27.590	27.623	27.750	27.516	27.413	27.540	27.373	27.694	27.580
S	66.397	64.966	65.722	65.723	64.286	65.676	65.120	64.520	64.152	65.356	65.093	66.449

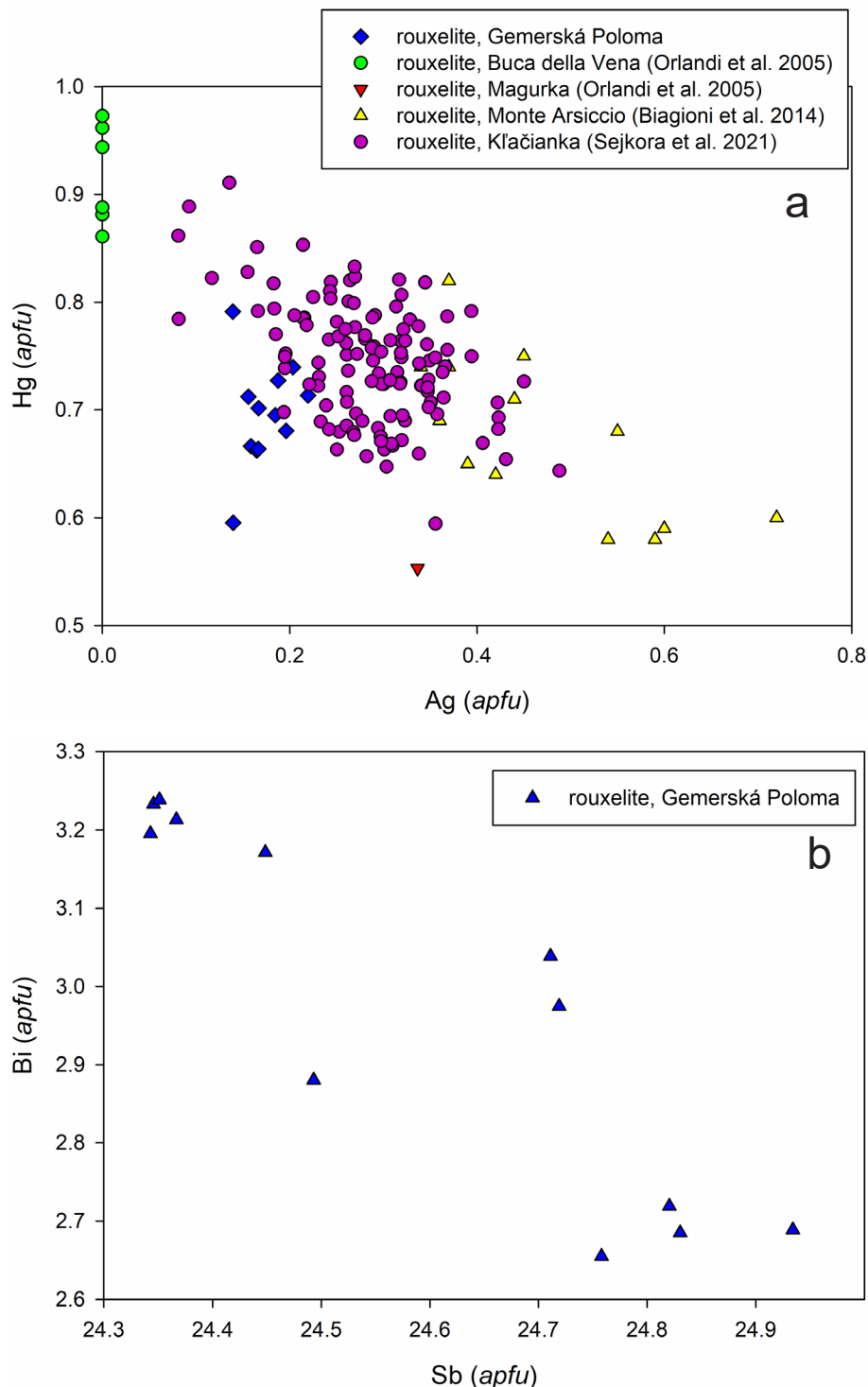
calculated empirical formulae are based on sum of *Me* = 53 *apfu*

#### 4.4. Rouxelite

Rouxelite is very rare. It forms subhedral to anhedral grains up to 80 µm (Fig. 13) directly associated with Bi-rich robinsonite, Bi-rich jamesonite and galena in quartz veins hosted in porphyric granite. Quantitative chemical analyses and the corresponding calculated empirical formulae of rouxelite from Gemerská Poloma

are shown in Tab. 7. Elevated contents of Ag (up to 0.22 apfu), which substitutes for Hg (Fig. 14a) as well as minor amounts of Fe (up to 0.12 apfu) were detected. The presence of significant contents of Bi (ranging from 2.66 to 3.24 apfu) substituting for Sb (Fig. 14b) is a characteristic feature of rouxelite from Gemerská Poloma, whereas no Bi was detected in rouxelite from

Buca della Vena and Magurka (Orlandi et al. 2005) or Kl'ačianka (Sejkora et al. 2021) and rouxelite from Monte Arsicio (Biagioni et al. 2014) shows only minor bismuth enrichment (up to 0.03 apfu). The mean ( $n = 12$ ) empirical formula of studied rouxelite based on  $\Sigma Me = 53$  apfu is  $(Cu_{1.95}Fe_{0.04})_{\Sigma 1.99}(Hg_{0.70}Ag_{0.17})_{\Sigma 0.87}Pb_{22.58}(Sb_{24.59}Bi_{2.97})_{\Sigma 27.56}S_{65.28}$ .



#### 4.5. Bouronite

Bouronite was rarely found as anhedral grains and aggregates up to 40 µm in size associated with tintinaite and galena (Fig. 15) in quartz veins hosted in porphyric granite. WDS analyses of bouronite from Gemerská Poloma are shown in Tab. 8. Besides of dominant contents of Pb, Cu, Sb and S only minor amounts of Bi (up to 0.03 apfu) were observed (Fig. 10). The mean ( $n = 7$ ) empirical formula of studied bouronite based on the sum of all atoms = 6 is  $Pb_{0.97}Cu_{0.95}(Sb_{1.02}Bi_{0.02})_{\Sigma 1.04}S_{3.04}$ .

#### 4.6. Tetrahedrite group minerals (tetrahedrite-(Zn), tetrahedrite-(Fe))

Minerals of the tetrahedrite group are very rare and occur only in quartz veins hosted in porphyric granite. They form anhedral grains and aggregates up to 7 mm in size embedded in quartz, closely associated with chalcopyrite and pyrite. Quantitative chemical analyses and the corresponding calculated empirical formulae of minerals of the tetrahedrite group from Gemerská Poloma are shown in Tab. 9. The trigonal position is predominantly occupied by Cu and only mi-

**Fig. 14a** – Variation of Ag vs. Hg contents (apfu) in rouxelite from Gemerská Poloma and other worldwide occurrences. **b** – Variation of Sb versus Bi contents (apfu) in rouxelite from Gemerská Poloma.

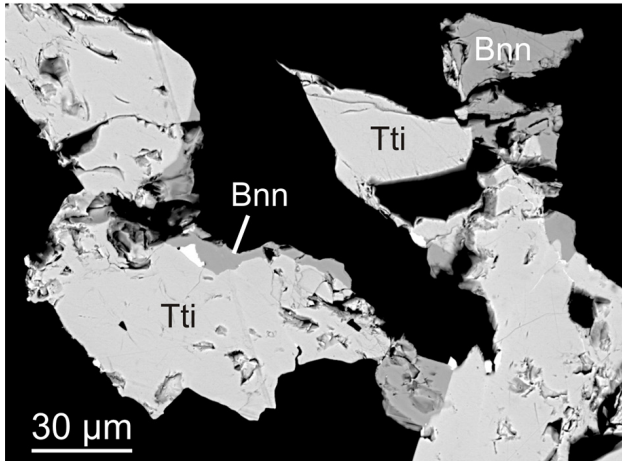


**Fig. 15** Bournonite (Bnn) associated with tintinaite (Tti) and galena (white) in quartz (black). Sample GPA5, BSE image.

nor amounts of Ag (up to 0.10 *apfu*) are present. Zinc is a dominant element in the tetrahedral site (reaching up to 1.18 *apfu*), but Fe (reaching up to 1.16 *apfu*) is locally prevailing over Zn (Fig. 16), accompanied by only minor amounts of Hg (up to 0.05 *apfu*). Antimony is considerably prevailing (3.55–4.08 *apfu*) over As (0.03–0.58 *apfu*), so according to the recently published nomenclature scheme of minerals of the tetrahedrite group (Biagioli et al. 2020), the studied phases from Gemerská Poloma correspond to tetrahedrite-(Zn) and tetrahedrite-(Fe).

**Tab. 8** Chemical composition of bournonite from Gemerská Poloma (in wt. %)

	GPA5							
Pb	41.38	41.74	41.71	41.15	41.29	40.82	41.62	
Cu	12.47	12.39	12.07	12.45	12.46	12.22	12.43	
Sb	25.88	25.59	25.21	25.91	25.62	24.80	25.80	
Bi	0.06	0.98	1.19	0.25	0.53	1.14	0.71	
S	19.96	20.10	20.10	19.90	19.88	19.82	20.36	
total	99.75	100.80	100.28	99.66	99.78	98.81	100.91	
Pb	0.973	0.976	0.981	0.969	0.973	0.972	0.967	
Cu	0.956	0.945	0.926	0.956	0.957	0.949	0.941	
Sb	1.036	1.018	1.009	1.039	1.028	1.004	1.020	
Bi	0.001	0.023	0.028	0.006	0.012	0.027	0.016	
Σ	1.037	1.041	1.037	1.045	1.040	1.031	1.036	
S	3.033	3.038	3.056	3.030	3.029	3.049	3.056	

calculated empirical formulae are based on sum of all atoms = 6 *apfu*

#### 4.7. Origin and metallogenetic setting of the studied mineralization

Bismuth (especially bismuthinite derivates and kobellite homologs) and lead–antimony sulfosalts (especially jamesonite, boulangerite or bournonite) are relatively common ore minerals at the siderite-type hydrothermal carbonate–quartz veins with sulfides hosted in Paleozoic (mostly Carboniferous) rocks in the Spišsko-gemerské rудohorie Mts. (e.g., Varček 1957; Kupčík et al. 1969; Grecula et al. 1995; Pršek 2008; Mikuš et al. 2018,

**Tab. 9** Chemical composition of tetrahedrite-(Zn) and tetrahedrite-(Fe) from Gemerská Poloma (in wt. %)

	GPS8									
	Ttr-Fe			Ttr-Zn						
Ag	0.65	0.65	0.67	0.62	0.62	0.58	0.53	0.42	0.43	0.45
Cu	37.85	37.73	37.15	37.51	37.40	37.19	37.51	37.41	38.00	38.01
Fe	3.70	3.90	3.87	2.68	2.62	2.70	2.71	2.76	3.13	3.08
Zn	3.42	3.16	3.21	4.52	4.50	4.52	4.52	4.65	4.26	4.27
Hg	0.24	0.04	0.20	0.38	0.65	0.29	0.24	0.54	0.57	0.52
Sb	29.63	29.49	29.50	29.40	29.34	29.34	29.25	29.44	26.46	26.76
As	0.19	0.15	0.17	0.29	0.35	0.42	0.33	0.64	2.64	2.50
S	24.55	24.47	24.32	24.52	24.36	24.34	24.30	23.91	24.41	24.35
total	100.23	99.59	99.09	99.92	99.84	99.38	99.39	99.78	99.89	99.93
$\Sigma$ Cu <sub>A</sub> site	6.000	6.000	6.000	6.000	6.000	6.000	6.000	6.000	6.000	6.000
Cu <sub>B</sub> site	3.852	3.872	3.797	3.834	3.820	3.794	3.852	3.748	3.778	3.781
Ag	0.100	0.100	0.104	0.096	0.096	0.090	0.082	0.064	0.065	0.068
$\Sigma$ B site	3.952	3.972	3.901	3.930	3.916	3.884	3.934	3.812	3.843	3.849
Fe	1.096	1.161	1.161	0.800	0.783	0.809	0.810	0.818	0.916	0.901
Zn	0.865	0.803	0.823	1.152	1.148	1.157	1.154	1.178	1.066	1.067
Hg	0.020	0.003	0.017	0.032	0.054	0.024	0.020	0.045	0.047	0.042
$\Sigma$ C site	1.981	1.968	2.001	1.983	1.985	1.990	1.984	2.041	2.028	2.011
Sb	4.025	4.027	4.060	4.023	4.021	4.032	4.009	4.005	3.553	3.594
As	0.042	0.033	0.038	0.064	0.078	0.094	0.074	0.142	0.575	0.546
$\Sigma$ D site	4.067	4.060	4.098	4.087	4.099	4.126	4.083	4.147	4.129	4.140
S	12.664	12.688	12.710	12.740	12.676	12.702	12.648	12.351	12.446	12.420

calculated empirical formulae are based on sum of *Me* = 16 *apfu*

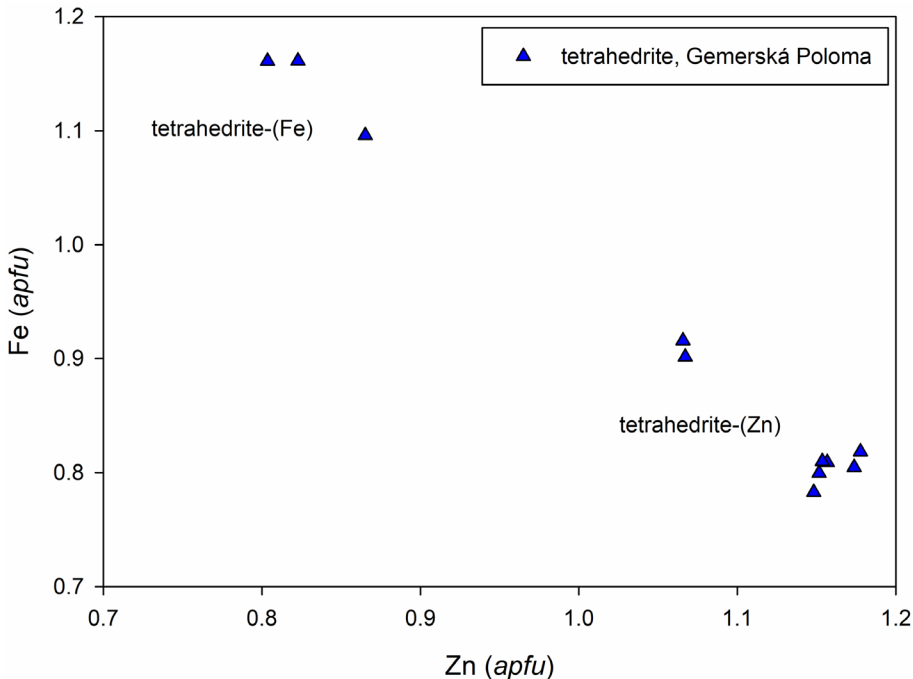


**Fig. 16** Variation of Zn and Fe contents (apfu) in minerals of the tetrahedrite group from Gemerská Poloma.

2019). Although the studied association of sulfosalts from the hydrothermal quartz veins at the Gemerská Poloma has many similarities with the sulfosalt mineralization frequently developed at the siderite-type hydrothermal veins in the Gemicic unit, it represents considerably different and much older type of mineralization. Kohút and Stein (2005) confirmed the Permian (~260 Ma) age of hydrothermal ore mineralization related to the Hnilec granite intrusion by Re/Os dating of molybdenite. In contrast, recent geochronological data from hydrothermal monazite (Hurai et al. 2015) or hydrothermal carbonates and gersdorffite (Kiefer et al. 2020) support the Cretaceous age of the siderite-type hydrothermal veins in the Gemicic unit. Moreover, bismuthinite, kobellite homologs and Bi-rich jamesonite were recently identified at hydrothermal U–Mo mineralization in Majerská valley near Čučma, also directly related to Permian Gemicic granites (Ferenc et al. 2021). Thus, the association of sulfosalts represented by bismuthinite, kobellite homologs and Bi-rich Pb–Sb sulfosalts is not typical only for the siderite-type veins but also for the other, mineralogically different and older types of hydrothermal mineralization in the Gemicic unit.

The origin of the hydrothermal quartz veins with sulfosalts at the Gemerská Poloma is connected to the post-magmatic hydrothermal activity directly related with the intrusion of specialized, P-, F- and Li-enriched S-type Gemicic granites. This is supported by the fact that the studied veins are developed strictly in granitic rocks as well as by significantly different styles of mineralization with an abundant presence of fluorite or phosphates

(Števko et al. 2015) and locally also Nb–Ta minerals (Uher et al. 2009) or bastnäsite-(Ce) (Števko et al. 2020) and only minor presence of hydrothermal carbonates (Mn-rich siderite and minor dolomite). Hurai ed. (2007) studied fluid inclusions in quartz and fluorite from the hydrothermal quartz veins with sphalerite, galena and Pb–Sb sulfosalt hosted in granite from the exploration drill hole VDD-14 located in Dlhá dolina near Gemerská Poloma. Homogenization temperatures of primary two-phase  $H_2O-CO_2$  inclusions in quartz were 115–150 °C and  $H_2O-NaCl-CaCl_2$  fluid inclusions in fluorite homogenized at 96–147 °C. The salinities varied substantially (from 3.1 to 35 wt. % NaCl eq.), especially in fluid inclusions in fluorite. It can be assumed that the studied hydrothermal quartz veins with sulfosalts, fluorite and phosphates from Gemerská Poloma represent relatively low thermal, granite-related hydrothermal mineralization.

## 5. Conclusions

The hydrothermal quartz veins hosted in S-type Gemicic granites at Elisabeth mine near Gemerská Poloma contain an interesting and complex association of Bi, Pb–Bi and Pb–Sb sulfosalts represented by bismuthinite derivates, minerals of kobellite homologous series, boulangerite, robinsonite, jamesonite, rouxelite, bournonite and minerals of the tetrahedrite group.

The two distinct types of sulfosalts associations were distinguished, each related to the different type of host rock and with variable Bi/Sb ratio. The first one is represented predominantly by Bi-rich sulfosalts (bismuthinite

derivates, kobellite, giessenite–izoklakeite) and it is characteristic for the quartz veins hosted in P-enriched leucogranite. In the second association, developed only in hydrothermal quartz veins hosted in porphyric granites, both Bi (bismuthinite derivates) as well as significant amounts of Sb-rich sulfosalts (tintinaite, boulangerite, robinsonite, jamesonite, rouxelite, bournonite and tetrahedrite-(Zn) to tetrahedrite-(Fe)) are present.

The origin of the hydrothermal quartz veins with sulfosalts at the Gemerská Poloma is connected to the post-magmatic hydrothermal activity directly related with the intrusion of Permian, specialized, S-type Gemicic granites.

**Acknowledgements.** This work was financially supported by the VEGA project (2/0028/20) to MŠ and by the Ministry of Culture of the Czech Republic (DKRVO 2019-2023/1.II.c, 00023272) to JS. Both referees, Juraj Majzlan and Štefan Ferenc, as well as handling editor Jiří Zachariáš and editor-in-chief Jakub Plášil, are highly acknowledged for comments and suggestions that helped immensely to improve the manuscript.

Supplementary file with tables containing chemical analyses of bismuthinite derivates, kobellite-tintinaite series, giessenite-izoklakeite series, boulangerite, robinsonite and jamesonite is available online at the Journal web site (<http://dx.doi.org/10.3190/jgeosci.328>).

## References

- ARMBRUSTER T, HUMMEL W (1987) (Sb,Bi,Pb) ordering in sulfosalts: crystal-structure refinement of a Bi-rich izoklakeite. *Amer Miner* 72: 821–831
- BAJANÍK Š, IVANIČKA J, MELLO J, PRISTAŠ J, REICHWALDER P, SNOPKO L, VOZÁR J, VOZÁROVÁ A (1984) Geological map of the Slovenské Rudohorie Mts. – eastern part 1 : 50 000. Dionýz Štúr Institute of Geology, Bratislava
- BIAGIONI C, MOËLO Y, ORLANDI P (2014) Lead–antimony sulfosalts from Tuscany (Italy). XV. (Tl–Ag)-bearing rouxelite from Monte Arsiccio mine: occurrence and crystal chemistry. *Mineral Mag* 78: 651–661
- BIAGIONI C, GEORGE LL, COOK NJ, MAKOVICKY E, MOËLO Y, PASERO M, SEJKORA J, STANLEY CJ, WELCH MD, BOSI F (2020) The tetrahedrite group: Nomenclature and classification. *Amer Miner* 105(1): 109–122
- BREITER K, BROSKA I, UHER P (2015) Intensive low-temperature tectono-hydrothermal overprint of peraluminous rare-metal granite: a case study from the Dlhá dolina valley (Gemicicum, Slovakia). *Geol Carpath* 66: 19–36
- BROSKA I, UHER P (2001) Whole-rock chemistry and genetic typology of the West-Carpathian Variscan granites. *Geol Carpath* 52: 79–90
- BROSKA I, KUBIŠ M (2018) Accessory minerals and evolution of tin-bearing S-type granites in the western segment of the Gemicic Unit (Western Carpathians). *Geol Carpath* 59: 483–497
- CIOBANU CL, COOK NJ (2000) Intergrowths of bismuth sulphosalts from the Ocna de Fier Fe-skarn deposit, Banat, Southwest Romania. *Eur J Mineral* 12: 899–917
- COOK NJ (1997) Bismuth and bismuth-antimony sulphosalts from Neogene vein mineralisation, Baia Borșa area, Maramureş, Romania. *Mineral Mag* 61: 387–409
- COOK NJ, CIOBANU CL (2003) Lamellar minerals of the cuprobismutite series and related padéraite: A new occurrence and implications. *Canad Mineral* 41: 441–456
- DIANIŠKA I, BREITER K, BROSKA I, KUBIŠ M, MALACHOVSKÝ P (2002) First phosphorous-rich Nb–Ta–Sn-specialised granite from the Carpathians – Dlhá dolina valley granite pluton, Gemicic superunit. *Geol Carpath* 53: Special Issue (CD-ROM)
- DIANIŠKA I, UHER P, HURAI V, HURAIROVÁ M, FRANK W, KONEČNÝ P, KRÁL J (2007) Mineralization of rare-metal granites. Pp. 254–330 In: HURAI V, ED. (2007) Sources of fluids and origin of mineralizations in the Gemicic unit. Open file report, Dionýz Štúr Institute of Geology, Bratislava, 1–365 (in Slovak)
- DRNZÍKOVÁ L, MANDÁKOVÁ K (1982) Mineralogy of tin and associated mineralizations in Hnilec ore field. Unpublished report, Geofond, 1–90 (in Slovak)
- FERENC Š, ŠTEVKO M, MIKUŠ T, MILOVSKÁ S, KOPÁČIK R, HOPPANOVÁ E (2021) Primary minerals and age of the hydrothermal quartz veins containing U–Mo–(Pb, Bi, Te) mineralization in the Majerská valley near Čučma (Gemicic Unit, Spišsko-gemerské rudohorie Mts., Slovak Republic). *Minerals* 11: 629
- GRASER S, HARRIS DC (1986) Giessenite from Giessen near Binn, Switzerland: New data. *Canad Mineral* 24: 19–20
- GRECULA P, ABONYI A, ABONYIOVÁ M, ANTAŠ J, BARTALSKÝ B, BARTALSKÝ J, DIANIŠKA I, ĐUĐA R, GARGULÁK M, GAZDAČKO L, HUDÁČEK J, KOBULSKÝ J, LÖRINCZ L, MACKO J, NÁVESŇÁK D, NÉMETH Z, NOVOTNÝ L, RADVANEC M, ROJKOVIČ I, ROZLOŽNÍK L, VARČEK C, ZLOCHA Z (1995) Mineral deposits of the Slovak Ore Mountains. Vol. 1. Geocomplex, Bratislava, 1–834
- HARRIS DC, ROBERTS AC, CRIDDLE AJ (1986) Izoklakeite, a new mineral species from Izok Lake, Northwest Territories. *Canad Mineral* 24: 1–5
- HURAI V, ED. (2007) Sources of fluids and origin of mineralizations in the Gemicic unit. Open file report, Dionýz Štúr Institute of Geology, Bratislava, 1–365 (in Slovak)
- HURAI V, PAQUETTE JL, LEXA O, KONEČNÝ P, DIANIŠKA I (2015) U–Pb–Th geochronology of monazite and zircon in albitite metasomatites of the Rožňava–Nadabula ore field (Western Carpathians, Slovakia): implications for the origin of hydrothermal polymetallic siderite veins. *Mineral Petrol* 109: 519–530

- JAMBOR JL, LACHANCE GR (1968) Bismuthian robinsonite. *Canad Mineral* 9: 426–428
- KIEFER S, ŠTEVKO M, VOJKO R, OZDÍN D, GERDES A, CREASER RA, SZCZERBA M, MAJZLAN J (2020) Geochronological constraints on the carbonate–sulfarsenide veins in Dobšiná, Slovakia: U/Pb ages of hydrothermal carbonates, Re/Os age of gersdorffite, and K/Ar ages of fuchsite. *J Geosci* 65: 229–247
- KILÍK J (1997) Geological characteristic of the talc deposit in Gemerská Poloma–Dlhá dolina. *Acta Montan Slovaca* 2: 71–80 (in Slovak)
- KOHÚT M, STEIN H (2005) Re–Os molybdenite dating of granite-related Sn–W–Mo mineralisation at Hnilec, Gemic Superunit, Slovakia. *Mineral Petro* 85: 117–129
- KUBIŠ M, BROSKA I (2005) The role of boron and fluorine in evolved granitic rock systems (on the example of the Hnilec area, Western Carpathians). *Geol Carpath* 56: 193–204
- KUBIŠ M, BROSKA I (2010) The granite system near Betliar village (Gemic Superunit, Western Carpathians): evolution of a composite silicic reservoir. *J Geosci* 55: 131–148
- KUPČÍK V, SCHNEIDER A, VARČEK C (1969) Chemical composition of some Bi sulfosalts from the Spišsko-gemerské rudoohorie Mts. *Neu Jb Mineral, Mh* 10: 445–454 (in German)
- MAKOVICKY E, KARUP-MØLLER S (1986) New data on giessenite from the Bjørkåsen sulfide deposit at Otoften, northern Norway. *Canad Mineral* 24: 21–25
- MAKOVICKY E, MAKOVICKY M (1978) Representation of composition in the bismuthinite–aikinite series. *Canad Mineral* 16: 405–409
- MAKOVICKY E, MUMME WG (1986) The crystal structure of izoklakeite,  $Pb_{51.3}S_{20.4}Bi_{19.5}Ag_{1.2}Cu_{2.9}S_{114}$ : the kobellite homologous series and its derivates. *Neu Jb Mineral, Abh* 153: 121–145
- MALACHOVSKÝ P (1983) Mineralogy and paragenetic conditions of tin, rare metal and hydrothermal mineralization in Dlhá dolina. Unpublished report, Geofond, 1–146 (in Slovak)
- MALACHOVSKÝ P, JELEŇ S, ĎUĎA R (1997) Minerals of indium from Gemerská Poloma–Dlhá dolina. *Natura Carpat* 38: 17–22 (in Slovak)
- MALACHOVSKÝ P, UHER P, ĎUĎA R (2000) Nb–W minerals in Dlhá valley rare-element granites, Spiš-Gemer Ore Mountains, Slovakia. *Natura Carpat* 41: 17–22 (in Slovak)
- MIKUŠ T, KONDELA J, JACKO S, MILOVSKÁ S (2018) Garavelite and associated sulphosalts from the Strieborná vein in the Rožňava ore field (Western Carpathians). *Geol Carpath* 69: 221–236
- MIKUŠ T, BAKOS F, HÖNIG S (2019) Bismuth sulphosalts from the siderite–sulphidic and As–Co mineralization in Medzov area, Slovakia. *Ageos* 11(2): 91–102
- MOËLO Y, ROGER G, MAUREL-PALACIN D, MARCOUX E, LAROUSSI A (1995) Chemistry of some Pb–(Cu,Fe)–(Sb,Bi) sulfosalts from France and Portugal. Implications for the crystal chemistry of lead sulfosalts in the Cu-poor part of the  $Pb_2S_2$ – $Cu_2S$ – $Sb_2S_3$ – $Bi_2S_3$  system. *Mineral Petro* 53: 229–250
- MOËLO Y, MAKOVICKY E, MOZGOVA NN, JAMBOR JL, COOK N, PRING A, PAAR W, NICKEL EH, GRAESER S, KARUP-MØLLER S, BALIC-ZUNIC T, MUMME WG, VURRO F, TOPA D, BINDI L, BENTE K, SHIMIZU M (2008) Sulfosalt systematics: a review. Report of the sulfosalt subcommittee of the IMA Commission on Ore Mineralogy. *Eur J Mineral* 20: 7–46
- ORLANDI P, MOËLO Y, MEERSCHAUT A, PALVADEAU P, LÉONE P (2005) Lead–antimony sulfosalts from Tuscany (Italy). VIII. Rouxelite,  $Cu_2HgPb_{22}Sb_{28}S_{64}(O,S)_2$ , a new sulfosalt from Buca della Vena mine, Apuan Alps: definition and crystal structure. *Canad Mineral* 43: 919–933.
- OZAWA T, SAITOW A, HORI H (1998) Chemistry and crystallography of Bi-rich izoklakeite from the Otome mine, Yamanashi Prefecture, Japan and discussion of the izoklakeite–giessenite series. *Mineral J* 20: 179–187
- PAŽOUT R (2020) Distribution of Bi in the crystal structure of Bi-rich jamesonite,  $FePb_4(Sb_{5.48}Bi_{0.52})_{\Sigma 6}S_{14}$ . *J Geosci* 65: 261–265
- PAŽOUT R, SEJKORA J, ŠREIN V (2017) Bismuth and bismuth–antimony sulphosalts from Kutná Hora vein Ag–Pb–Zn ore district, Czech Republic. *J Geosci* 62: 59–76
- PETRASOVÁ K, FARYAD SW, JEŘÁBEK P, ŽÁČKOVÁ E (2007) Origin and metamorphic evolution of magnesite–talc and adjacent rocks near Gemerská Poloma, Slovak Republic. *J Geosci* 52: 125–132
- PETRÍK I, KOHÚT M (1997) The evolution of granitoid magmatism during the Hercynian orogen in the Western Carpathians. In: GRECULA P, HOVORKA D, PUTIŠ M (eds.) *Geological Evolution of the Western Carpathians*. Miner Slov Monogr 235–252
- PETRÍK I, KUBIŠ M, KONEČNÝ P, BROSKA I, MALACHOVSKÝ P (2011) Rare phosphates from the Surovec topaz–Li mica microgranite, Gemic unit, Western Carpathians, Slovak Republic: Role of  $F/H_2O$  of the melt. *Canad Mineral* 49: 521–540
- POLLER U, UHER P, BROSKA I, PLAŠIENKA D, JANÁK M (2002) First Permian–Early Triassic zircon ages for tin-bearing granites from the Gemic unit (Western Carpathians, Slovakia): connection to the post-collisional extension of the Variscan orogen and S-type granite magmatism. *Terra Nova* 14: 41–48
- POUCHOU JL, PICHOIR F (1985) “PAP” ( $\phi\phi Z$ ) procedure for improved quantitative microanalysis. In: ARMSTRONG JT (ed) *Microbeam Analysis*. San Francisco Press 104–106
- PRŠEK J (2008) Chemical composition and crystal chemistry of Bi sulfosalts from the hydrothermal mineralizations hosted in crystalline basement of the Western Carpathians. Univerzita Komenského, Bratislava, 1–108 (in Slovak)

- PRŠEK J, MIKUŠ T (2006) Bi sulphosalts from the Lúbietová-Kolba occurrence. *Miner Slov* 38: 159–164
- PRŠEK J, OZDÍN D, SEJKORA J (2008) Eclarite and associated Bi sulfosalts from the Brezno-Hviezda occurrence (Nízke Tatry Mts, Slovak Republic). *Neu Jb Mineral, Abh* 185: 117–130
- RADVANEC M, GONDA S (2019) Genetic model of Permian hydrothermal mineralization in Gemicic unit (W. Carpathians) from deep-seated zone of anatetic melting to volcanic-exhalative SedEx mineralization on surface. *Miner Slov* 52: 109–156
- RADVANEC M, KODĚRA P, PROCHASKA W (2004) Mg replacement at the Gemerská Poloma talc–magnesite deposit, Western Carpathians, Slovakia. *Acta Geol Sin* 20: 773–790
- RADVANEC M, KONEČNÝ P, ONDREJKA M, PUTIŠ M, UHER P, NÉMETH Z (2009) The Gemicic granites as an indicator of the crustal extension above the Late-Variscan subduction zone during the early Alpine riftogenesis (Western Carpathians): an interpretation from the monazite and zircon ages dated by CHIME and SHRIMP methods. *Miner Slov* 41: 381–394
- SEJKORA J, ŠTEVKO M, PRŠEK J, LITOCHLEB J, HOVORIČ R, MAKOVICKY E, CHOVAR M (2021) Unique association of sulfosalts from the Kláčianka occurrence, Nízke Tatry Mts., Slovak Republic. *Minerals*, 11, 1002
- ŠTEVKO M, SEJKORA J (2017) Boulangerite and robinsonite from the Ochtiná-Čížko baňa occurrence (Slovak Republic). *Bull Mineral Petrolog* 25: 273–276 (in Slovak)
- ŠTEVKO M, UHER P, SEJKORA J, MALÍKOVÁ R, ŠKODA R, VACULOVÍČ T (2015) Phosphate minerals from the hydrothermal quartz veins in specialized S-type granites, Gemerská Poloma (Western Carpathians, Slovakia). *J Geosci* 60: 237–249
- ŠTEVKO M, SEJKORA J, UHER P, CÁMARA F, ŠKODA R, VACULOVÍČ T (2018) Fluorarrojadite-(BaNa), Ba<sub>4</sub>Na<sub>4</sub>CaFe<sub>13</sub>Al(PO<sub>4</sub>)<sub>11</sub>(PO<sub>3</sub>OH)F<sub>2</sub>, a new member of the arrojadite group from Gemerská Poloma, Slovakia. *Mineral Mag* 82: 863–876
- ŠTEVKO M, SEJKORA J, DOLNÍČEK Z (2020) Hydrothermal bastnäsite-(Ce) from the Elisabeth adit near Gemerská Poloma (Slovak Republic). *Bull Mineral Petrolog* 28: 1–8 (in Slovak)
- TOPA D, MAKOVICKY E, PAAR WH (2002) Composition ranges and exsolution pairs for the members of the bismuthinite–aikinite series from Felbertal, Austria. *Canad Mineral* 40: 849–869
- UHER P, BROSKA I (1996) Post-orogenic Permian granitic rocks in the Western Carpathian–Pannonian area: geochemistry, mineralogy and evolution. *Geol Carpath* 47: 311–321
- UHER P, MALACHOVSKÝ P, BAČÍK P, CHUDÍK P, ŠTEVKO M (2009) Polycrase-(Y), uranopolycrase a Ti–Nb–Ta–Fe mineral in quartz veins and exocontact zones of the Gemicic granites, the Slovak Ore Mountains. *Bull mineral-petrolog Odd Nár Muz (Praha)* 17: 14–24 (in Slovak)
- VARČEK C (1957) Summary of paragenetic conditions of ore deposits in Gemer region. *Geol Práce, Zoš* 46: 107–131 (in Slovak)
- VILLASEÑOR G, CATLOS EJ, BROSKA I, KOHÚT M, HRAŠKO L, AGUILERA K, ETZEL TM, KYLE R, STOCKLI DF (2021) Evidence for widespread mid-Permian magmatic activity related to rifting following the Variscan orogeny (Western Carpathians). *Lithos* (390–391): 106083
- VOUDOURIS PC, SPRY PG, MAVROGONATOS C, SAKELLARIS GA, BRISTOL SK, MELFOS V, FORNADEL AP (2013) Bismuthinite derivates, lillianite homologues, and bismuth sulfotellurides as indicators of gold mineralization in the Stanos shear-zone related deposit, Chalkidiki, northern Greece. *Canad Mineral* 51: 119–142
- WAGNER T, JONSSON E (2001) Mineralogy of sulfosalt-rich vein-type ores, Boliden massive sulfide deposit, Skellefte District, Northern Sweden. *Canad Mineral* 39: 855–872
- XIANG-PING G, WANATABE M, OHKAWA M, HOSHINO K, SHIBATA Y, DESONG C (2001) Felbertalite and related bismuth sulfosalts from the Feniushan copper skarn deposit, Nanjing, China. *Canad Mineral* 39: 1641–1652
- ZAKRZEWSKI MA, MAKOVICKY E (1986) Izoklakeite from Vena, Sweden, and the kobellite homologous series. *Canad Mineral* 24: 7–18